Assessing vegetation degradation using high-resolution satellites in the region of Lake Manyara

Kevin Hamann

Utrecht University

Assessing vegetation degradation using high-resolution satellites in the region of Lake Manyara

MSc Thesis, GEO4-1520, 37.5 ECTS

April 2022

Author: Kevin Hamann
Student number: 5893577
E-mail: k.t.hamann@students.uu.nl

First supervisor: Geert Sterk/Steven de Jong
Second supervisor: Steye Verhoeve

MSc programme: Earth, Surface and Water
Faculty of Geosciences
Department of Physical Geography
Utrecht University

Cover page photo, source: https://www.flickr.com/photos/manyara_ranch_conservancy/16213211932/in/album-72157650087785966/

Abstract

This thesis aims to assess vegetation degradation in the region of Lake Manyara in Northern Tanzania over the years 2017 until 2021. Multiple studies concluded that the LULC is changing around Lake Manyara over the past years. In some cases, this is due to humans, while in other cases it is suggested that it is due to vegetation degradation. Previous studies showed high vegetation resilience and no signs of vegetation degradation, yet the Maasai observed a change in vegetation. Vegetation changes are observed in similar areas, these changes are changes from high-nutritious grasses to low-nutritious grasses and bush encroachment. The assessment is done with the high-resolution satellites, Sentinel-2 and PlanetScope, with soil moisture data from SMAP and precipitation data from CHIRPS 2.0. The indices for the assessment are NDVI, GCC, MBI and NDWI. This thesis concluded that precipitation and infiltration were not simultaneously, infiltration occurred later. Vegetation did not start growing simultaneously with precipitation, but with infiltration in the subsurface. The lack of infiltration could be due to that crusting is affecting the vegetation in the area. Crusting results in less infiltration and less growth of grasses, while shrubs and trees are less affected by crusting. This result is in line with bush encroachment and is a good indication that vegetation degradation might occur in the grassland and savannah areas around Lake Manyara. Vegetation resilience is still high, although vegetation does not start to grow when the precipitation starts. Vegetation starts to grow when water infiltrates the subsurface.

Table of Contents

1 Introduction

1.1 Background information

Lake Manyara is located in northern Tanzania and is part of the East African Rift System (EARS). The EARS is characterized by highlands and lowlands. The highlands are more densely vegetated and have a sub-humid climate, while the lowlands have a semi-arid climate (Cooke et al., 2007; Kimaro et al., 2018) and are characterized by widespread open or bushed grasslands and rangelands (savannah) (Kimaro et al., 2018). The climate in northern Tanzania is influenced by the seasonal shift of the Intertropical Convergence Zone (ITCZ) resulting in two dry and two wet seasons (Deus et al., 2013). The vegetation in the savannah areas around Lake Manyara is well adapted to the seasonal rainfall and appears to be highly resilient (Verhoeve et al., 2021). However, this good resilience can be disrupted due to climatic and human impacts, such as more frequent droughts and increased grazing pressure by Maasai livestock herds.

The Maasai are a Nilotic ethnical group living a pastoral or agro-pastoral life in the rangelands of northern Tanzania and southern Kenya (Homewood et al., 2009; McCabe et al., 2010). In the past, the Maasai had a fully nomadic life and relocated their bomas (Maasai settlement with houses and livestock) if the rangelands did not provide enough food (McCabe et al., 2010). The Maasai are not able to live their full nomadic life anymore, because of Tanzanian regulations, urbanization and an increase in agricultural lands (Goldman, 2011). The present grazing areas are under extreme grazing pressure because the Maasai only have a limited area for grazing around their bomas (Fratkin, 2001; Goldman, 2011). This increasing grazing pressure may result in vegetation degradation and could have an impact on the grazing capability of the Maasai livestock.

1.2 The problem

1.2.1 Vegetation degradation in northern Tanzania

Vegetation degradation will be described in this thesis as the negative change between different types of vegetation where the new vegetation is not usable, e.g. as food for livestock or humans, or as the change from vegetation to bare lands (Sterk & Stoorvogel, 2020). The area around Lake Manyara has undergone changes in land-use and land-cover (LULC) (Homewood et al., 2009), which is observed by multiple remote sensing (RS) studies. The RS studies of Kiunsi and Meadows (2006), van den Bergh (2016), van Rosmalen (2021), Verhoeve (2019), and Wynants et al. (2018) had different and conflicting results because of fluctuations in changing vegetation types over the years. These studies could be biased due to the use of limited datasets, climatic factors and classification errors (Conroy, 2001; Degen, 2015; Iqbal & Khan, 2014; Maerker et al., 2015). Droughts are lowering the vegetation cover during the year of the drought. However, the vegetation cover quickly recovers after a normal or wet year following a drought. This indicates that vegetation resilience is high in northern Tanzania (Verhoeve et al., 2021).

A high resilience suggests that vegetation recovers quickly during periods of water abundance (Sterk & Stoorvogel, 2020). However, it is possible a shift to more drought-prone vegetation types may occur, which might result in less favourable vegetation that is not preferred by livestock. The shift between different types of vegetation, where the new vegetation is not consumable as food for humans or livestock, is called vegetation degradation (Sterk & Stoorvogel, 2020). A vegetation shift from nutritious grasses to low nutritious grasses is already noticed in the Ngorongoro conservation area (Niboye, 2010) and around the town of Selela (Oba & Kaitira, 2006), resulting in less available food for livestock. The change in vegetation from grasslands to bushlands or forests is observed in many parts of Africa (Stevens et al., 2017; Venter et al., 2018), this is called bush encroachment. Bush encroachment is found in many savannah areas in North Tanzania (H.

S. Kimaro & Treydte, 2021; Mtui et al., 2017) or similar areas in South Kenya (Li et al., 2020). These types of vegetation degradation may affect the Maasai livestock grazing opportunities.

According to an interview with the local Maasai, the availability or quality of grass is reducing and the amount of trees is increasing (Verhoeve, 2019). The Maasai perspective is in line with the findings of bush encroachment (Kimaro & Treydte, 2021; Li et al., 2020) and grass type shifting (Niboye, 2010; Oba & Kaitira, 2006). The Maasai think the reason for the decrease in grass cover is due to livestock grazing pressure, an increase of trees, a decrease in rainfall, or fire (Verhoeve, 2019).

Crusting could also be a reason for vegetation degradation. Since it could both stimulate and prevent vegetation growth (Assouline et al., 2015). Crusting can occur on most soils, except for soils with high coarse sand and very low silt and clay contents (Bradford & Huang, 1992). Crusting has a large impact on infiltration, e.g. a thin crust of 0.1 mm can reduce infiltration by a factor of 1800 (McIntyre, 1958). There are two types of crusting that might be influencing vegetation growth in this area, biological and physical. The biological crusting is due to drought, this starts a mechanism that eventually releases nutrients and is beneficial for the vegetation (Belnap et al., 2005; Hawkes, 2003; Mayland & McIntosh, 1966; Mills & Fey, 2004). The physical crusting is due to precipitation (Assouline et al., 2015) or the trampling of cattle or other animals (Mills & Fey, 2004). It is observed that bare or grazed areas are more prone to crusting than vegetated areas since the soil in bare areas or grasslands is more affected by direct sunlight and precipitation (Assouline et al., 2015; Kidron et al., 2017; Mills & Fey, 2004).

Crusting is common in savannah areas and can lead to specific vegetation patterns due to the different effects of crusting on vegetation, e.g. the moving banded vegetation patterns like the tiger bush patterns (Lefever & Lejeune, 1997; Thiery et al., 1995; Valentin & D'Herbès, 1999). In tiger bush patterns the moving direction has beneficial crusting for vegetation, while the other side has a negative crusting effect on the vegetation (Valentin & D'Herbès, 1999).

Crusting is observed around Lake Manyara, in Manyara Ranch, in a photo of Verhoeve (2019) and is shown in figure 1. However, this study was not conducted to observe crusting, thus more information about crusting in the area is not found.

Figure 1; Crusting is as the cracks in between small patches of grass. The location of this photo is inside Manyara Ranch ROI, south of Makuyuni. The photo was taken as a field observation by Verhoeve (2019).

1.2.2 Remote sensing and vegetation degradation

Spatial-temporal monitoring of the savannah is challenging due to the fine-scale heterogeneity (Pickett et al., 2003) and high resilience (Cooke et al., 2007; Verhoeve et al., 2021). Previous RS studies with a coarse spatial resolution had less accurate results than with a high spatial resolution, e.g. the Landsat classification of Verhoeve (2019) or Kiunsi and Meadows (2006). These types of classification are more suitable for more homogeneous areas (Li et al., 2020). Many worldwide RS studies to monitor vegetation degradation used coarse resolution satellites, like Landsat (Hadeel et al., 2012; Kiunsi & Meadows, 2006) or EO-1 Hyperion (Lyu et al., 2020). Hadeel et al. (2012) and Kiunsi & Meadows (2006) found vegetation degradation over a long time period by studying vegetation change and Lyu et al. (2020) found vegetation degradation in a single year by studying vegetation health with hyperspectral data. The advantage of these satellites is their hyperspectral sensors to obtain more spectral information, the downside is their low spatial resolution. Van Rosmalen (2021) used high-resolution Sentinel-2 imagery with Landsat imagery, this resulted in better classification. However, it was not conducted to monitor vegetation degradation for the fine-scaled heterogeneity of the savannah.

Cheng et al. (2020) concluded that both Sentinel-2 and PlanetScope images will result in good and comparable Normalized Difference Vegetation Index (NDVI) results. They were able to distinguish and classify vegetation types on the Kenyan rangelands.

Li et al. (2020) monitored vegetation degradation in the Greater Maasai Mara Ecosystem in Kenya, which is a similar semi-arid savannah area as in North Tanzania. They used Sentinel-2 and Worldview-3 to study the area with high-resolution classification. They observed a decrease in grassland and an increase in woody vegetation, i.e., bush encroachment, from 2016 to 2018.

The vegetation degradation will be assessed with the use of vegetation indices (VIs). The VIs used are the normalized difference vegetation index or NDVI (Rouse et al., 1973; Tucker, 1979), modified bare soil index or MBI (Nguyen et al., 2021), green chromatic colour or GCC (Gillespie et al., 1987), normalized difference water index or NDWI (Gao, 1996), subsurface soil moisture or SuSM (*Subsurface Soil Moisture (Corrected with SMAP Imagery)*, n.d.), and the surface soil moisture or SSM (*Surface Soil Moisture (Corrected with SMAP Imagery)*, n.d.).

The NDVI is able to provide a quantity of vegetation and an approximation of vegetation health and cover. If there is a decline in NDVI over time, it could be an indication of vegetation degradation (Hadeel et al., 2012; Meneses-Tovar, 2011; Yengoh et al., 2014). The GCC indicates vegetation greenness, this is used to indicate vegetation browning. The amount of greenness of browning is an indicator of vegetation degradation (Runnström et al., 2019). The MBI uses the lack of vegetation to indicate bare soils. If this index increases, more bare soil will occur and thus less vegetation, and more vegetation degradation. Water is indicated with high values of the NDWI, it is used to classify water correctly (Hadeel et al., 2012). The SSM approximates the surface soil moisture content and the SuSM approximates the subsurface soil moisture content. A combination of SuSM and SSM is used to indicate droughts of water abundant periods.

1.3 Objectives

The aim of this thesis is to assess vegetation degradation in the Monduli district using RS images. To achieve the aim of this thesis, it is divided into objectives.

I. Finding multiple proper study areas with different grazing policies around Lake Manyara;
II. Exploring the collected RS imagery to obtain the best possible vegetation degradation assessments in the selected study areas;
III. Using vegetation index analysis to assess vegetation degradation in the selected study areas

2 Study area

2.1 Region of Interest

Three regions of interest (ROIs) were selected based on three different grazing policies, while still having similar vegetation types. The locations of the three ROIs are given in figure 2. The three ROIs are all located in the Lake Manyara Catchment. The Lake Manyara Catchment is a closed basin with a terminal lake (Compen, 2021; Keijzer, 2020), called Lake Manyara, and is located in northern Tanzania. Thus, Lake Manyara has no outlet, which contributes to a fluctuating lake area over different seasons and years. Lake Manyara has an area of 410 km² at the low levels and 480 km² at the high levels (Yanda & Madulu, 2005).

2.1.1 Manyara Ranch

Manyara Ranch is a conservation area east of Lake Manyara and southwest of the town of Makuyuni and has its longitudes between 3°27' S and 3°40' S and its latitudes between 35°56' E and 36°06' E. It is an area of 178.07 km² (Goldman, 2011). The ROI from the Manyara Ranch is the Ranch and an expansion of the area surrounding the town of Makuyuni, it has an area of 195.40 km². The elevation of the ROI variates between 990 meters and 1,080 meters asl.

Until the late 1990s, the ranch was a state-run cattle ranch. When that ended, the area was used as a part-time, regulated, expansion of the Maasai villages of Esilalei and Oltukai (Goldman, 2011). With the part-time expansion of the Maasai villages the Manyara Ranch obtained a new land-use objective, it became a conservation area. This results in part-time grazing by cattle and letting nature be nature. The Maasai are allowed to graze in these fields, however under specific policies (Goldman, 2011).

The vegetation in Manyara Ranch consists mainly of bushed grasslands and open grasslands or savannah (AWF, 2003; Manyara Ranch Conservancy, 2019). The Makuyuni river system in the Manyara Ranch is an unstable seasonal river that leads to much erosion in the surrounding area (AWF, 2003; Egberts, 2020).

This ROI is chosen because this is a savannah area with conservation rules where the Maasai are allowed to graze. This gives an insight into how the Maasai can graze with a view on how the vegetation is less disturbed by human actions.

2.1.2 Selela area

The town of Selela is located approximately 30 km north of Manyara Ranch and 20 km northeast of Mto wa Mbo. The ROI has its longitudes between 3°11' S and 3°17' S and its latitudes between 35°55' E and 36°02' E. The borders of the ROI are the highlands in the Northeast, the riverbed going south from the highlands is the Western border, the riverbed going east while bending to the south are the Northern and Eastern borders, and the Southern border is chosen arbitrarily not to obtain a too large ROI. The ROI has an area of 107.83 km² and its elevation variates between 980 meters and 1,080 meters asl.

The town of Selela is mainly a Maasai town, where many villagers live an agro-pastoral lifestyle (Oba & Kaitira, 2006). The vegetation is mainly savannah, bushed savannah and small and scattered agricultural fields.

This ROI is chosen because it is a savannah area where the Maasai are grazing. In this area, all human activities are allowed (Shechambo, 2018). According to Kiunsi & Meadows (2006), there are many degraded soil areas in the area around the town of Selela. This makes it a good ROI to study how the Maasai need to treat the area and how the vegetation will react to it.

2.1.3 Lake Manyara National Park

Lake Manyara National Park (LMNP) is located directly west of Lake Manyara and southwest of Mto wa Mbo. LMNP is home to a combination and variety of landforms and

vegetation types which create a unique ecosystem (UNESCO, 2019). The LMNP has an area of 648.7 km² (TANAPA, 2020). However, most of this area is home to unique vegetation, like groundwater forests or dense forests. These vegetation types are not comparable with the other ROIs and thus not usable for this thesis. The ROI is located in the north-northeast area of LMNP and follows the end of the lowland area of LMNP and part of the lake itself. The LMNP ROI has an area of 33.11 km² and its elevation variates between 950 meters and 1,020 meters asl. The ROI has its longitudes between 3°24' S and 3°32' S and its latitudes between 35°45' E and 35°51' E.

LMNP is a national park, which means there are no human activities, apart from tourism. The vegetation in the park is diverse and the vegetation in the ROI are grasslands, woodlands and lakeshore (UNESCO, 2019). The unique groundwater forest in the LMNP is not in the ROI, because no other ROI has a comparable area.

This ROI is chosen because of its undisturbed vegetation, because of its protected status. Nobody is allowed to graze in the park and agriculture is also prohibited, thus no Maasai agriculture or livestock is allowed in the park. Since the ROI has comparable vegetation as the other ROIs without human interference, the ROI in LMNP is a suitable control group (Loth, 1999).

2.2 Climate

The study areas are in one of the driest areas in Tanzania and is characterized by a semi-arid climate. The study areas are around the city of Mto wa Mbo, which is located north of Lake Manyara. The climate is influenced by the seasonal shift of the ITCZ. This results in a bimodal precipitation pattern. The short rains (Vuli) occur between November and January, while the long rains (Masika) occur between February and May. The short and long rains can be interrupted by a short dry season in January and February. The long dry season is from June to October, and the length of it is dependent on the length of the start of the short rains and the end of the long rains (Deus et al., 2013).

Average rainfall ranges from approximately 500 mm/yr in the lowlands and up to 900 mm/yr in the highlands (Monduli District Council, 2021), and since the research areas are located in the lowlands, the average precipitation is between 400 mm/yr to 600 mm/yr

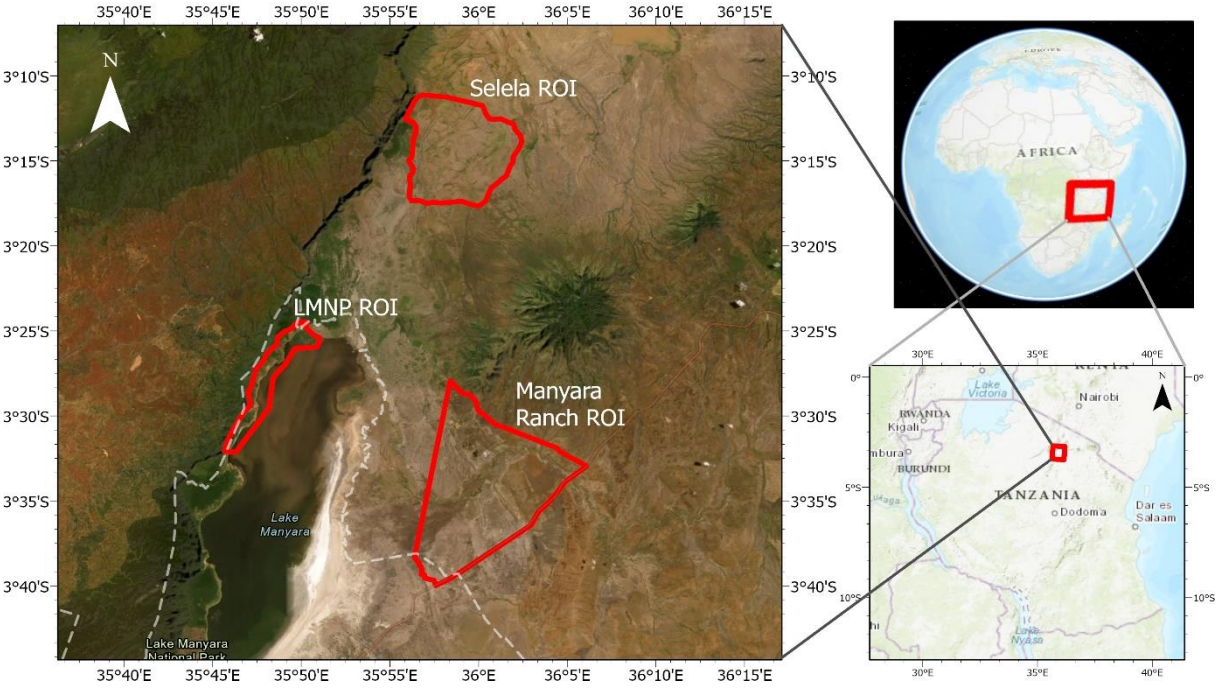

Figure 2; The study area map and the ROIs. The Selela ROI is the area with no conservation or grazing rules. The Manyara Ranch ROI is the conservation area where grazing is limited and under strict regulation. LMNP ROI is a national park where no human activities are allowed.

(Deus et al., 2013). The most precipitation is during March and April with monthly mean precipitation ranging from 50 mm/month to 280 mm/month and the driest months are July to September with a maximum monthly mean precipitation up to 20 mm/month (TMA, n.d.). This average yearly precipitation per month is seen in figure 3.

The daily average temperature in the district ranges between 14°C and 35°C (Deus et al., 2013; Monduli District Council, 2021). The warmest months are from December to February with monthly mean temperatures from 21°C to 25°C and the coldest months are from June to August with monthly mean temperatures from 18°C to 20°C (TMA, n.d.). The monthly mean range of temperatures is seen in figure 3.

3 Methods

This thesis uses high-resolution satellites to derive vegetation indices on a small pixel scale. Coarse satellites are used for a broad overview of water availability since field observations are limited in the study areas. The water availability is measured with precipitation and soil moisture, the latter is derived from radar images. The study period is from 2017 to 2021 because all satellites are in orbit during that period.

3.1 Vegetation degradation assessments

3.1.1 Indices

As a first vegetation degradation assessment, multiple index maps were created from the VIs. The explanation of these VIs and their formulas are shown in table 1. The NDVI and GCC were obtained from PlanetScope and Sentinel-2 bands, which are not directly similar. However, the bands are comparable, since the bands have overlapping bandwidths. The blue bandwidth is for both satellites between 459.4 and 515.0 nm, the green band is between 541.8 and 577.0 nm, the red band is between 649.5 and 670.0 nm and the NIR band is between 780.0 and 885.8 nm. Since the NDVI and GCC are derived from PlanetScope and Sentinel-2 bands, two maps of each of these indices are created. The MBI and NDWI are only obtained from Sentinel-2 bands since that is the only satellite with SWIR bands. The SuSM and SSM are obtained from the SMAP. Per year the statistics of the SuSM and SSM are calculated for analysis. The total amount of SuSM or SSM in the

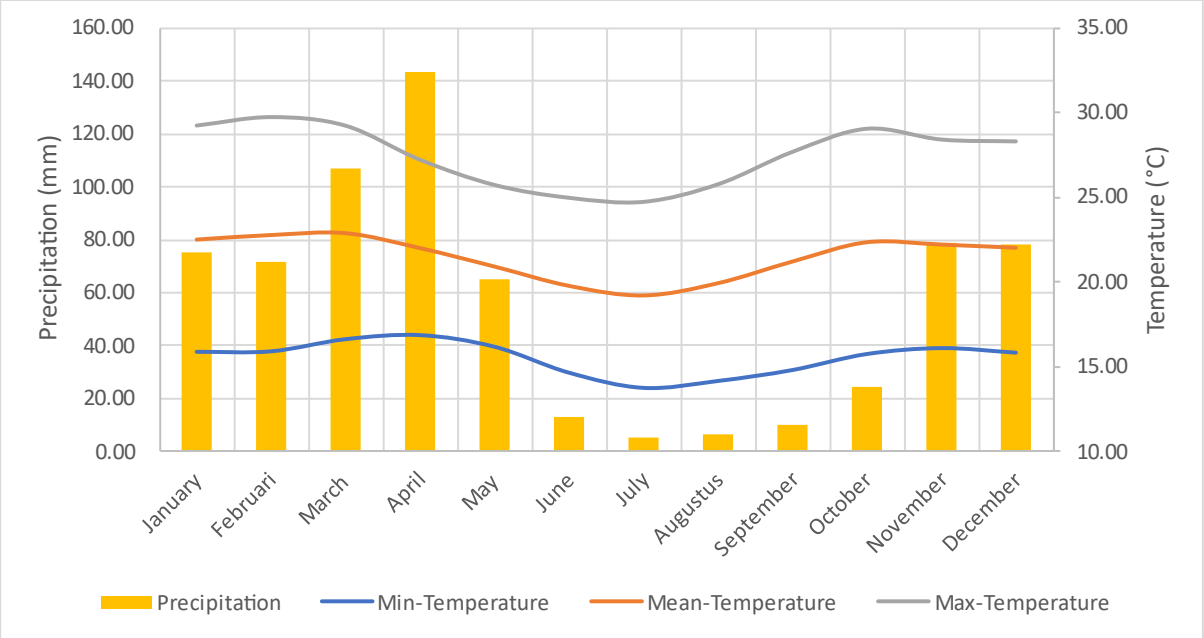

Figure 3; Monthly average climatology in the Arusha region from 1991-2020. The short rains are seen between November and January, the long rains are seen between February and May with the peak in April. During the long dry period between June and October almost no precipitation falls.
Source: https://climateknowledgeportal.worldbank.org/country/tanzania-united-republic/climate-data-historical

Table 1; The indices with their formulas and a short explanation; wavelengths of the colours: B (blue) = ±490 nm, G (Green) = ±560 nm, R (Red) = ±665 nm, NIR (near infrared) = ±865 nm, SWIR1 (shortwave infrared 1) = ±1610 nm, SWIR2 (shortwave infrared 2) = ±2195 nm.

Abbreviation	Name	Formula	Explanation
NDVI	Normalized Difference Vegetation Index	$\frac{NIR - R}{NIR + R}$	Quantities the living vegetation in an area, is between -1 and +1 (the more positive, the more vegetation).
MBI	Modified Bare Soil Index	$\frac{SWIR1 - SWIR2 - NIR}{SWIR1 + SWIR2 + NIR} + 0.5$	Indicates bare soil locations, is between -0.5 and +1.5 (bare soil is emphasized and received positive values until maxima).
GCC	Green chromatic coordinate	$\frac{G}{R + G + B}$	Indicates vegetation greenness, is between 0 and 1 (the higher the more green vegetation is).
NDWI	Normalized Difference Water Index	$\frac{NIR - SWIR2}{NIR + SWIR2}$	Indicator for vegetation liquid water content, is between -1 and +1 (the more positive, the more vegetation).

entire year is calculated, the number of days that the threshold is reached and the average amount of SuSM or SSM per day. The threshold for SuSM is 25 mm (*Subsurface Soil Moisture (Corrected with SMAP Imagery)*, n.d.) and for SSM is 10 mm (*Surface Soil Moisture (Corrected with SMAP Imagery)*, n.d.), below this amount the vegetation is not able to grow optimally (*Subsurface Soil Moisture (Corrected with SMAP Imagery)*, n.d.; *Surface Soil Moisture (Corrected with SMAP Imagery)*, n.d.). Days that reach the SuSM or SSM threshold are called respectively SuSM days or SSM days. The start of a new series of SuSM days is highlighted in the SuSM timeseries for each ROI. The same statistics are calculated for the precipitation. However, the threshold for precipitation is set at 1 mm, this is an arbitrary threshold and is because small precipitation events (below 1 mm) are ignored, since these days do barely contribute to water availability. Days that reach the threshold for precipitation are called rain days. The year in which the statistics are calculated are not normal calendar years, but a hydrological year is used. The periods are from January 2017 to July 2017 (2017), from August 2017 to July 2018 (2018), from August 2018 to July 2019 (2019), from August 2019 to July 2020 (2020) and from August 2020 to July 2021 (2021). Except for the start of 2017, all years start in the middle of the dry period. This means that the total water availability of 2017 could be biased while it is only a half hydrological year, since the end of 2016 is not taken into account. However, it does not affect the water availability at a moment in time.

Initially, only the indices from Sentinel-2 are used for the first vegetation assessment. For the first vegetation degradation assessment in a ROI, from each index, a mean time series of the whole ROI is plotted.

3.1.2 Change detection

The nine index maps and all the bands of three satellites are combined into one image stack map for each timestep for every ROI. Per ROI a multidimensional raster is created out of the image stack. This multidimensional raster is used to analyse change using the CCDC algorithm. CCDC stands for Continuous Change Detection and Classification and it is an unsupervised classification method based on a harmonic regression model that identifies abrupt changes in pixel values over time while accounting for long-term and seasonal change (Zhu & Woodcock, 2014). Thus, the CCDC algorithm should not detect resilience and seasonal vegetation changes as a change. This makes CCDC a proper change detection algorithm for detecting vegetation degradation. Other change detection algorithms, like

LandTrendr, may not be as effective as CCDC, since LandTrendr only detects annual and linear trends while CCDC detects monthly continuous trends. The output of this tool is a Cloud Raster Format with the analysis raster of the change detection data. This is a new multidimensional raster with an unspecified number of classes indicating different vegetation types and the rate of change in the vegetation types, or vegetation degradation. Thus, this already provides information about the changing areas, however, it does not provide information about what vegetation type is changing.

3.1.3 Specifying vegetation degradation and resilience

After CCDC, a change map is created. This map indicates the level and amount of change. From this map, interesting areas are chosen to study further. From each new specific area, it is made sure the vegetation type and land cover are uniform. Four areas are selected in Selela and Manyara Ranch and two areas are selected in LMNP.

In the selected new areas, the same assessment is done as the first assessment described in paragraph '3.1.1 Indices'. However, the indices from PlanetScope are added to the assessment. The difference between this second assessment with the first assessment is that this assessment is based on a single vegetation type and land cover and not over the whole ROI with different land covers and vegetation types.

3.1.4 Vegetation ROIs

After CCDC there are specific vegetation ROIs chosen inside of each ROI. Four vegetation ROIs were selected for Manyara Ranch and Selela and two vegetation ROIs were selected in LMNP.

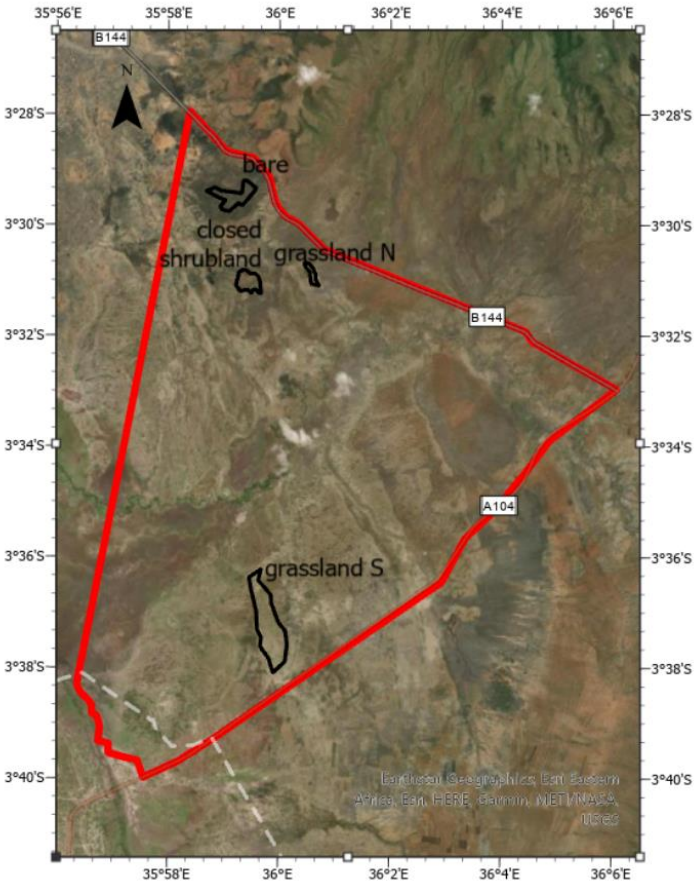

Figure 4; The 4 locations of the vegetation ROI inside Manyara Ranch ROI. There are 2 grasslands, one in the north (grassland N) and one in the south (grassland S), 1 closed shrubland and 1 area with a lot of erosion and gullies with little vegetation, only a few trees, this area is called bare for simplicity.

After CCDC, 4 areas had a special interest in Manyara Ranch. These 4 areas were 2 grasslands, one in the north (grassland N) and one in the south (grassland S), 1 closed shrubland and 1 area with a lot of erosion and gullies with little vegetation, only a few trees and was studied by Egberts (2020), this area was called bare for simplicity. The locations of these areas are seen in figure 4.

After CCDC, 4 areas had special interest in Selela. These four areas were 2 grasslands, one in the north (grassland N), which is around a boma, and one in the south (grassland S), which is not around a boma, 1 closed shrubland and 1 savannah area. The locations of these areas are seen in figure 5.

After CCDC,f 2 areas had a special interest in LMNP. These two areas are a forest area and closed shrubland. The locations of these areas are seen in figure 6.

3.2 Satellites

The satellites used for this thesis are the PlanetScope constellation, Sentinel-2, Soil Moisture Active Passive (SMAP) and CHIRPS 2.0, because of their high resolution and radar images. The study period is of a period from 2017 to 2021 in a selection of areas. The objective is to have one scene per ROI per month per satellite, the first scene of the month that qualifies best for this thesis is used.

The requirements of the image are:

- <20% cloud cover
- >90% ROI overlap from one moment of capture

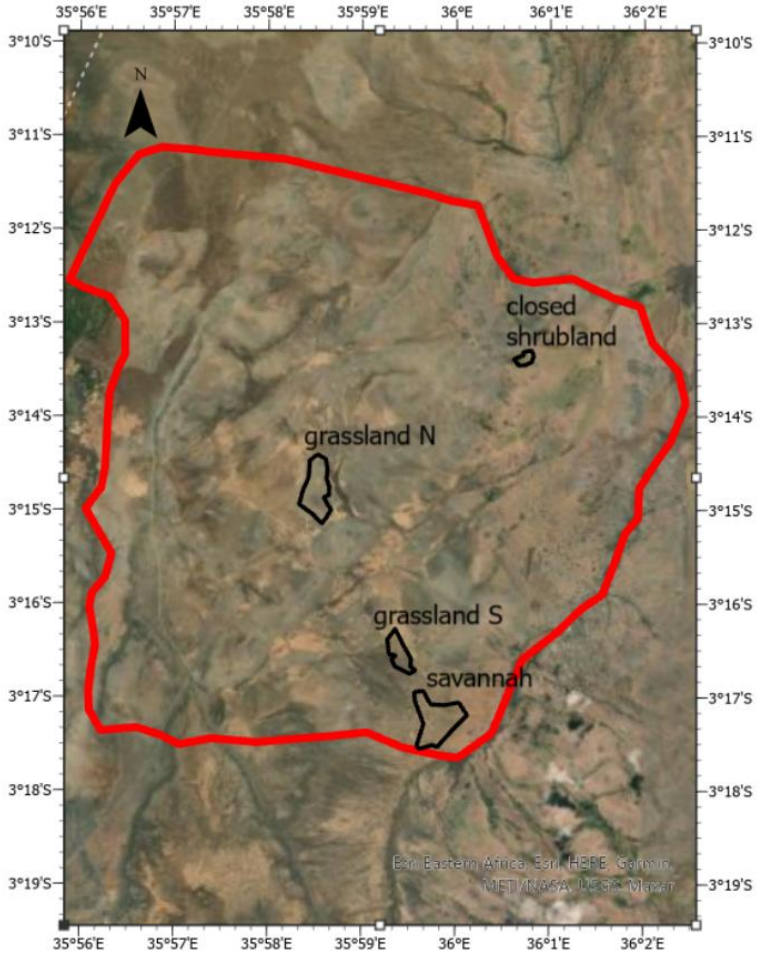

Figure 5; The 4 locations of the vegetation ROIs inside Selela ROI. There are 2 grasslands, one in the north (grassland N), which is around a boma, and one in the south (grassland S), which is not around a boma, 1 closed shrubland and 1 savannah area.

- Satellite specific requirements, which are explained in later sections of this paragraph

3.2.1 PlanetScope

Planet Labs started launching the PlanetScope mission in 2016. PlanetScope consists of a constellation of over 130 small Dove satellites collecting almost daily images of the entire land surface of the Earth with a resolution of 3 meters per pixel. This corresponds to a daily data collection capacity of 200 million km²/day (Planet, 2021).

PlanetScope is in a sun-synchronous orbit. There are three generations of sensors; the sensors on the Dove Classic (PS2) with an instrument capturing VNIR (visible/near-infrared) in 4 bands; the Dove-R (PS2.SD) with an instrument similar to PS2, but with an updated Bayer pattern and pass-band filters; and the SuperDove (PSB.SD) with an upgraded PS2.SD instrument with 8 bands. For this thesis, the PS2 is used and only if PS2 is not providing good quality images, the PS2.SD is used. The spectral ranges of the bands are given in table 2. PS2 images are used because of its very high spatial resolution of 3 by 3 meters, its NIR band and its continuous availability since 2017.

The image processing level of PlanetScope that is used is level 3B from the analytic 4-Band scenes. This provides a scene with Top of Atmosphere (TOA) radiance (Planet, 2021), which is a similar scene as the Sentinel-2 scenes.

3.2.2 Sentinel-2

The Sentinel-2 mission contains two polar-orbiting identical satellites in the same sun-synchronous orbit. Sentinel-2A was launched on 23 June 2015 and Sentinel-2B on 7 March

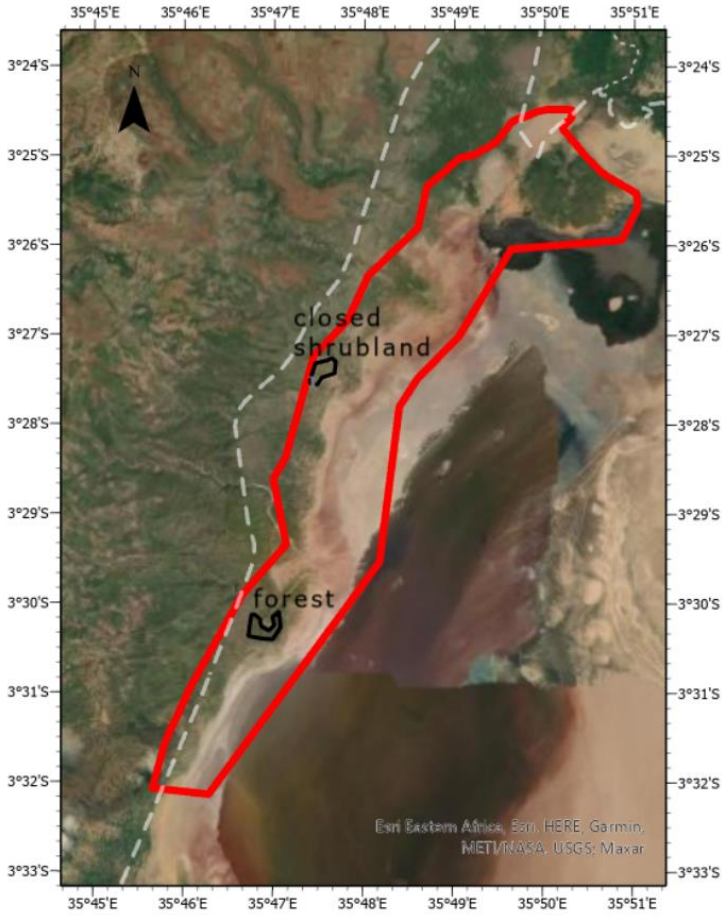

Figure 6; The 2 locations of the vegetation ROIs inside LMNP ROI. These are a forest area and closed shrubland.

Table 2; Wavelengths of the spectral bands of the PlanetScope sensors. The satellites from PlanetScope that are used are the Dove Classic (PS2) and the Dove-R (PS2.SD).

Spectral Band	PS2	PS2.SD
Band 1 (Blue)	455-515 nm	464-517 nm
Band 2 (Green)	500-590 nm	547-585 nm
Band 3 (Red)	590-670 nm	560-682 nm
Band 4 (NIR)	780-860 nm	846-888 nm

Table 3; Wavelengths of the spectral bands of both Sentinel-2 satellites and its spatial resolution.

Spectral band	Sentinel-2A	Sentinel-2B	Spatial resolution
Band 1 (Coastal aerosol)	432.2-453.2 nm	431.8-452.8 nm	60 m
Band 2 (Blue)	459.4-525.4 nm	459.1-525.1 nm	10 m
Band 3 (Green)	541.8-577.8 nm	541.0-577.0 nm	10 m
Band 4 (Red)	649.1-680.1 nm	649.5-680.5 nm	10 m
Band 5 (Vegetation Red Edge)	696.6-711.6 nm	695.8-711.8 nm	20 m
Band 6 (Vegetation Red Egde)	733.0-748.0 nm	731.6-746.6 nm	20 m
Band 7 (Vegetation Red Edge)	772.8-792.8 nm	769.7-789.7 nm	20 m
Band 8 (NIR)	779.8-885-8 nm	780.0-886.0 nm	10 m
Band 8a (Narrow NIR)	854.2-875.2 nm	853.0-875.0 nm	20 m
Band 9 (Water vapour)	9351-955.1 nm	932.7-953.7 nm	60 m
Band 10 (SWIR-Cirrus)	1358-1389 nm	1361.9-1391.9 nm	60 m
Band 11 (SWIR)	1568.2-1659.2 nm	1563.4-1657.4 nm	20 m
Band 12 (SWIR)	2114.9-2289.9 nm	2093.2-2278.2 nm	20 m

2017. The two satellites are phased at 180° to each other. Each satellite has a revisit time of 10 days at the equator, which results in a 5-day revisit time for the Sentinel-2 mission with the two satellites (ESA, n.d.-c).

The Sentinel-2 satellites provide multispectral imagery at high to coarse spatial resolution (10 to 60 m). The main instrument of the Sentinel-2 mission is the Multispectral Instrument (MSI). The MSI has 13 spectral bands ranging from VNIR to SWIR (short-wave infrared) (ESA, n.d.-b). The specifications of the MSI and its spectral bands are seen in table 3. The Sentinel-2 images are used because of its high spatial resolution in VNIR and its multispectral capability.

For this thesis, the product type of the data used from Sentinel-2 is level-1C, this is the TOA reflectance in cartographic geometry (ESA, n.d.-a), which is a similar scene as the PlanetScope scenes.

3.2.3 SMAP

The Soil Moisture Active Passive, or SMAP for short, is a radar satellite from NASA, the USDA, NOAA and the USGS. The SMAP is specialised in monitoring soil moisture and freeze/thaw state of the surface (Entekhabi et al., 2010).

The soil moisture is estimated with a combined active and passive L-band radar with a frequency of 1.26 GHz and a resolution of 10 km (Entekhabi et al., 2010), the revisiting time is approximately 3 days and the SMAP has a global cover. Soil moisture consists of a Surface Soil Moisture (SSM) and Subsurface Soil Moisture (SuSM). The SSM consists of a depth of 25 mm in the soil (*Surface Soil Moisture (Corrected with SMAP Imagery)*, n.d.) and the SuSM has a depth of the root zone, which is approximately 275 mm (*Subsurface Soil Moisture (Corrected with SMAP Imagery)*, n.d.).

The average values of each ROI for the SuSM and SSM are products from the SMAP that are used in this thesis. These products are used to study the infiltration and water availability in the soil, which is important for vegetation to grow.

3.2.4 CHIRPS 2.0

The Climate Hazards group Infrared Precipitation with Stations (CHIRPS) dataset interpolates measured precipitation from (sparse) gauge stations and satellite means to

create a quasi-global (50°S-50°N), high resolution (0.05°), daily, pentadal, and monthly precipitation dataset (Funk et al., 2015). This dataset is used to create a gridded rainfall time series and can be used for trend analysis and seasonal drought monitoring.

From the second version of CHIRPS (CHIRPS 2.0) the average daily precipitation in each ROI was obtained.

4 Results

4.1 Manyara Ranch

4.1.1 Water availability

The water availability is a combination of SuSM, SSM and precipitation, it gives a proper indication of how water is available in the soil and how much fell during precipitation events per year. The SuSM time-series of Manyara Ranch is seen in figure 7. The SSM time-series of Manyara Ranch is seen in figure 8. The precipitation time-series of Manyara Ranch is seen in figure 9. All detailed information on the water availability of Manyara Ranch is seen in table 4.

In 2017 297.3 mm of rain fell over 28 days. These precipitation events resulted in a simultaneous increase in SuSM and SSM values. The precipitation that fell in 2017 was under the average.

The rains of 2018 start in October and it takes up to January for the SSM to reach its threshold. The SuSM reaches its threshold for a couple of days in November and December before reaching it for an extended period from January to July.

The start of the rains of 2019 was around November and resulted in minor peaks of the SSM and SuSM that did not reach the threshold. The threshold was reached in December for both SSM and SuSM. The precipitation this year had a similar quantity as in 2019. However, it was more scattered over fewer days. Thus the rains were more intense.

2020 was the year with the most water availability. When the rains started in October, the SuSM reached its threshold and did not go under it until June. The amount of precipitation that fell during that period was 1176.2 mm, this is almost double the average amount.

While the rains and the SuSM start around the same time, the SSM rarely reached its threshold. The SuSM kept moving around the threshold, while the rains were constant. There was 533.8 mm of rain that fell over 52 days.

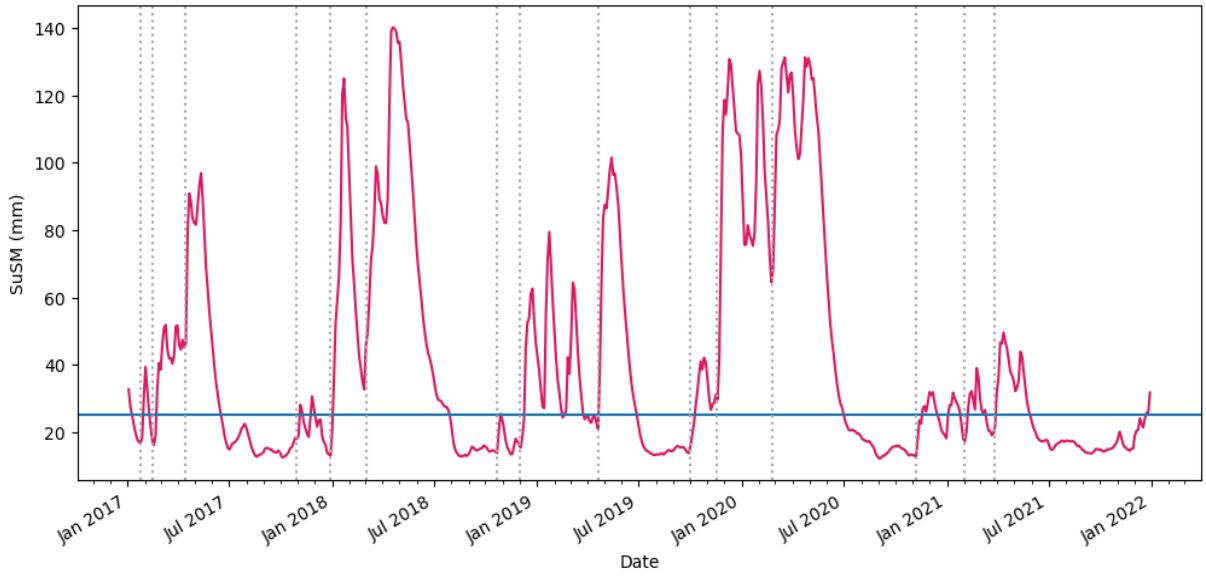

Figure 7; The averaged Subsurface Soil Moisture defined by the SMAP dataset of the Manyara Ranch ROI. The blue line indicates the threshold at 25 mm at which vegetation could be severely stressed. The onset of a strong increase in Subsurface Soil Moisture is represented by the vertical, grey-dotted lines.

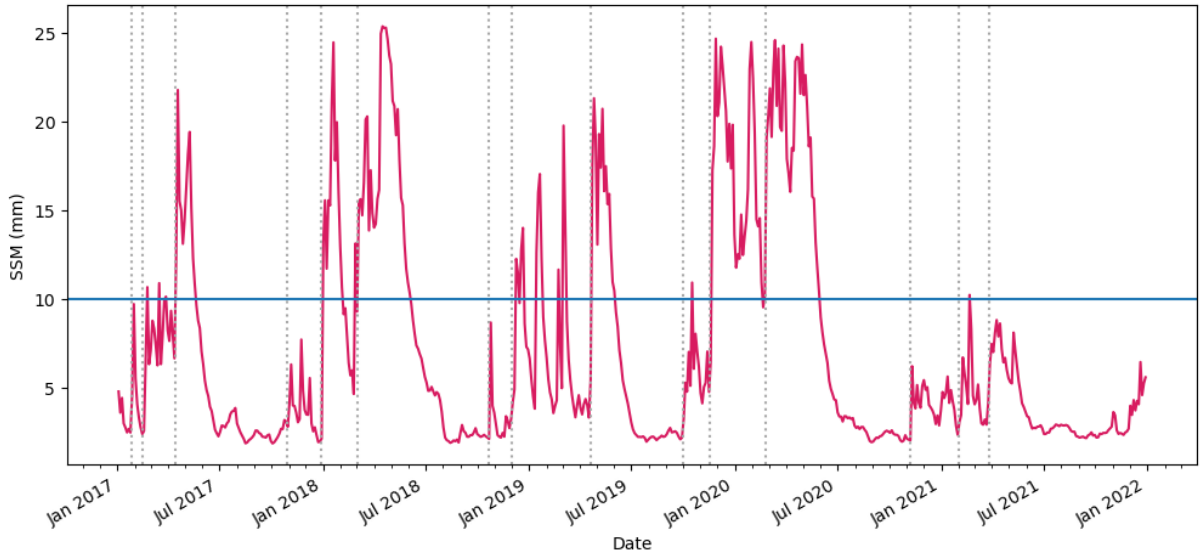

Figure 8; The averaged Surface Soil Moisture defined by the SMAP dataset of the Manyara Ranch ROI. The blue line indicates the threshold at 10 mm at which vegetation could be severely stressed. The onset of a strong increase in Subsurface Soil Moisture is represented by the vertical, grey-dotted lines.

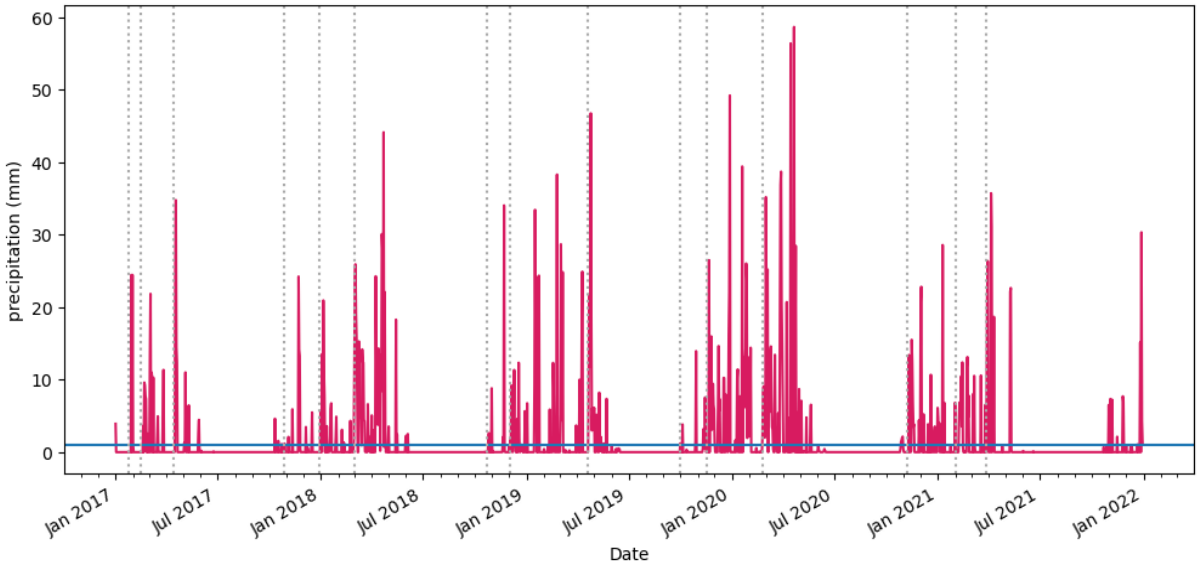

Figure 9; The averaged precipitation defined by the CHIRPS 2.0 dataset of the Manyara Ranch ROI. The blue line indicates the threshold at 1 mm at which precipitation does not contribute to Subsurface Soil Moisture. The onset of a strong increase in Subsurface Soil Moisture is represented by the vertical, grey-dotted lines.

4.1.2 The whole ROI

During the first overall vegetation degradation assessment of Manyara Ranch, VIs reacted after a peak in SuSM, which is shown as a dotted line in figure 10. The index pattern for NDVI and GCC was similar every year.

In 2017 there was a second-lowest peak in the NDVI and GCC, but the peak was very thin. The MBI showed a small dip in the graph, indicating less bare soil with a slow decline. The NDWI indicated a peak in water uptake from vegetation. All combined, it indicated a short and low intensity vegetation period in 2017.

The lowest peak of NDVI and GCC was in 2018, yet the period was long, namely 9 months. Indicating that there was much water available, which was also reflected in the SuSM, SSM and precipitation results. The first two peaks in SuSM only resulted in two small peaks in NDVI, GCC and NDWI, and only result in a small dip in MBI. The third SuSM peak resulted in the highest peak in NDVI and GCC during 2018. Yet, this third peak resulted in

Table 4; All indicators for water availability for all locations. The years are the hydrological years and all indicators are averaged over the respective ROI. The index days are the amount of days in a hydrological year that exceeded the threshold.

Location	Year	SuSM (mm/yr)	SuSM days	SSM (mm/yr)	SSM days	Precipitation (mm/yr)	Rain days	Precipitation (mm/rain day)
Manyara Ranch	2017	2824.0	132	490.9	45	297.3	28	10.6
	2018	6105.1	219	1079.3	132	670.6	73	9.2
	2019	4191.9	177	756.7	75	639.2	59	10.8
	2020	8193.9	267	1425.2	192	1176.2	97	12.1
	2021	2816.0	144	468.8	3	533.8	52	10.3
Selela	2017	1456.1	72	249.2	3	281.7	33	8.5
	2018	5703.2	186	1060.4	123	591.8	62	9.5
	2019	3980.0	144	731.3	84	545.4	48	11.4
	2020	7416.9	219	1346.9	180	1065.2	86	12.4
	2021	3210.3	168	553.9	9	469.8	52	9.0
LMNP	2017	1699.9	81	257.1	3	338.8	32	10.6
	2018	8644.7	240	1260.3	165	726.0	72	10.1
	2019	6426.1	285	949.2	108	720.0	60	12.0
	2020	11094.2	255	1601.6	201	1172.5	96	12.2
	2021	2847.3	105	416.1	0	584.5	53	11.0

the highest peak of NDWI and dip in MBI, reaching almost zero, during all 5 study years. All combined, it resulted in a long, but low intensity vegetation period with lots of surface water and little bare soil in 2018. The high water availability was seen as the highest peak in SuSM and SSM.

2019 was the third highest peak for NDVI and GCC. However, the NDVI was relatively higher than the GCC peak. The reaction to an input of water, seen as a SuSM peak, was fast and properly noticeable. The timing of the first rains resulted in a high peak in all indices and a dip in MBI and the second rains resulted in a lower peak and dip than the

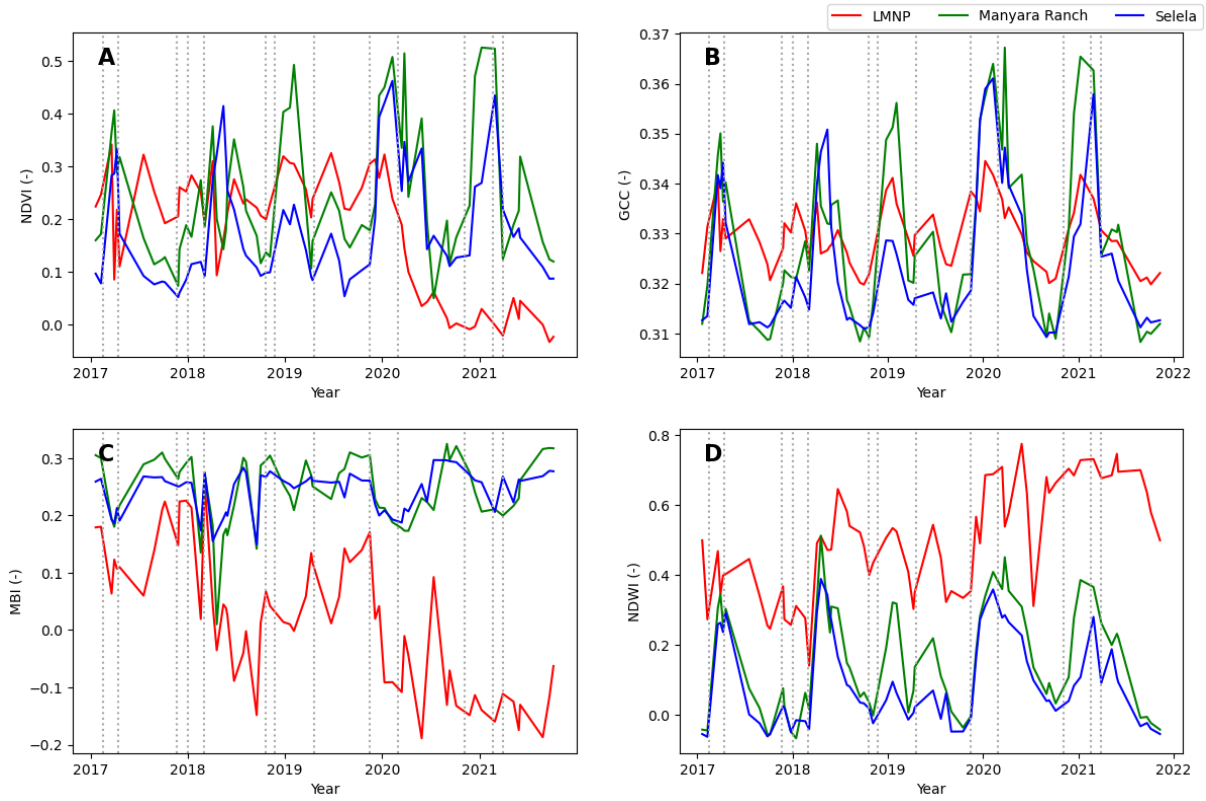

Figure 10; The VI graphs for LMNP, Manyara Ranch and Selela. (A) Indicates the NDVI derived from Sentinel-2, (B) indicates the GCC derived from Sentinel-2, (C) indicates the MBI derived from Sentinel-2 and (D) indicates the NDWI derived from Sentinel-2. The onset of a strong increase in Subsurface Soil Moisture is represented by the vertical, grey-dotted lines.

first rains. The amount of precipitation during 2019 (639.2 mm) was similar to 2018 (670.6 mm). However, the amount of SuSM (4191.9 mm) and SSM (765.7 mm) are much lower in 2019 than the SuSM (6105.1 mm) and SSM (1079.3 mm) in 2018. Yet the NDVI and GCC values indicated higher VI values in 2019 than in 2018.

2020 had the most water availability of all years during the study period. This coincided with a wide and second-highest NDVI peak and the highest GCC peak. The dip in MBI was the highest and very wide and the NDWI was wide and the second highest. All the peaks and the MBI dips were directly after the increase in SuSM. Thus, during 2020 there was much water availability for a long time, which was observed as the long and high VIs.

In 2021 the SuSM (2816.0 mm) and SSM (468.8 mm) were similar to the SuSM (2824.0 mm) and SSM (490.9 mm) amounts of 2017. However, the SSM days were much lower in 2021 (3 days) than in 2017 (45 days), this indicated there is more infiltration in 2021 than in 2017. Based on water availability, only 2017 was similar, all other years had more water availability than 2021. However, the NDVI peak was the highest peak of all study years, while the dip in MBI and the peaks in GCC and NDWI were only slightly smaller than, the very water abundant year, 2020. This indicated that 2021 was a high VI valued year with little water availability.

4.1.3 The 4 vegetation ROIs

The indices derived from Sentinel-2 and PlanetScope for these four areas are given in figure 11.

In 2017 no VI reaction was observed after the first SuSM peak and the first precipitation events. After a short dry period, the second SuSM peak ensured an increase in all VIs. This peak in VIs was the highest VI values during 2017. Closed shrubland reacted first and reached the highest VI values and grassland N also reacted to the SuSM peak, but to a

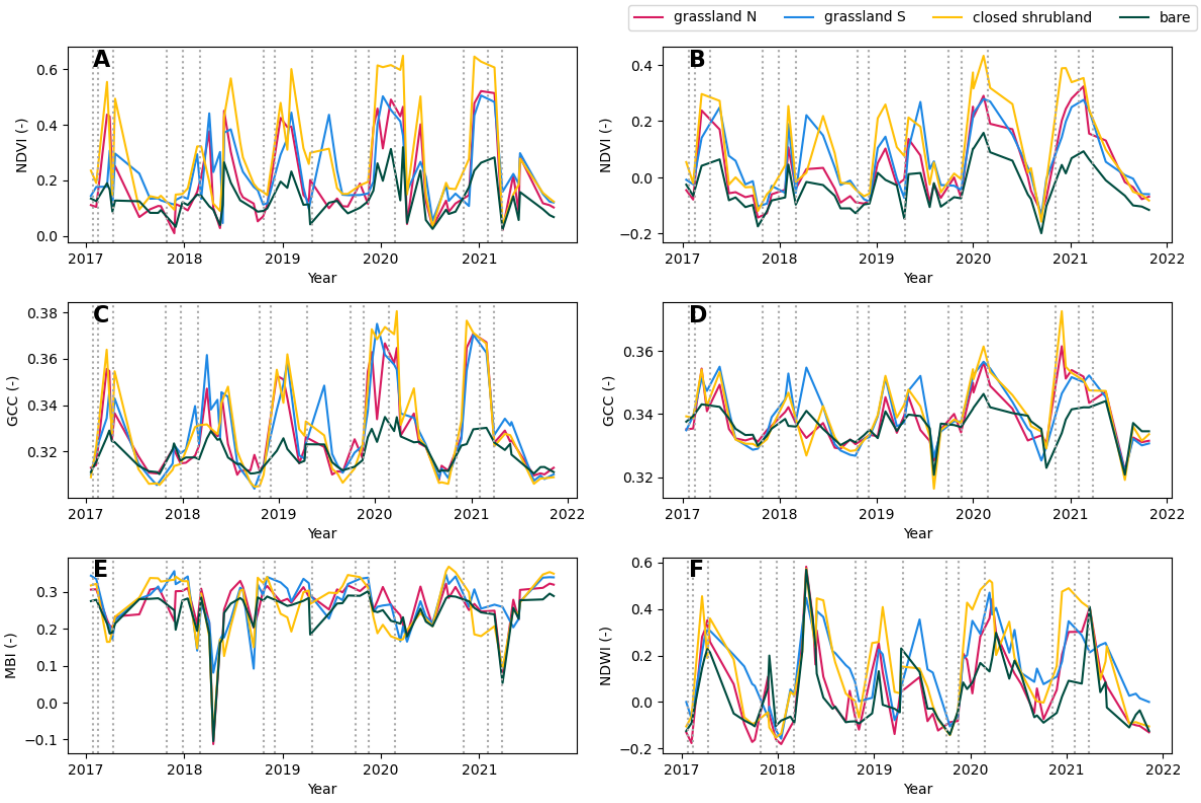

Figure 11; The VI graphs for grassland N, grassland S, closed shrubland and bare vegetation ROIs inside the Manyara Ranch ROI. (A) Indicates the NDVI derived from Sentinel-2, (B) indicates the NDVI derived from PlanetScope, (C) indicates the GCC derived from Sentinel-2, (D) indicates the GCC derived from PlanetScope, (E) indicates the MBI derived from Sentinel-2 and (F) indicates the NDWI derived from Sentinel-2. The onset of a strong increase in Subsurface Soil Moisture is represented by the vertical, grey-dotted lines.

lesser extent than closed shrubland. While looking at the Sentinel-2 NDVI and GCC grassland S had a small VI reaction and bare reacted even worse. While looking at the PlanetScope NDVI and GCC grassland S reacted still worse than grassland N, yet it reacted more compared to Sentinel-2 indices. The MBI indicated that there was a decrease in bare soil. The third SuSM peak resulted in a new lower VI peak, except for grassland according to the PlanetScope indices.

During the first SuSM peak of 2018, only little reaction in the VIs occurred. There was only a small dip in MBI for grassland N and bare and a peak in NDWI for the same locations. There was precipitation, yet the SuSM and SSM did not react to it. This means infiltration was not very high. Only after the second SuSM peak, the VIs reacted. Grassland S reacted the best to the water input, while the other three locations lacked a suspected peak. There was an enormous dip in MBI and a peak in NDWI for all locations. Indicating not much bare soil, but lots of water. Since there was a lot of water available, the vegetation remained longer with even a late VI peak for the closed shrubland. Grassland N had lower NDVI and GCC values than grassland S, but grassland S has a positive MBI and slightly less NDWI.

In 2019, the first SuSM peak did not respond with VI values increases for all areas. At the second SuSM peak all vegetation types showed an increase in VIs, whereas the bare area only has a small increase. The grassland S had higher VI values than the grassland N and the closed shrubland has the highest values. The third SuSM peak results in a slight increase in VI values for grassland N, closed shrubland and bare. While grassland S had a large increase in VI values after the third peak. All vegetation types had the same maximum VI values while comparing 2019 with 2018. However, the growing period (the period where VIs were reacting) was longer during 2019 compared to 2018. The peak during the growing period was months earlier in 2019 than in 2018. Yet, 2019 was a dryer year with less water availability than 2018.

Also, during the year with the highest water availability, 2020, vegetation did not respond to the first SuSM peak. After the second SuSM peak, the VIs increased rapidly. The bare area reached VI values higher than the VI values of grassland N during 2018 and 2019. The decline of VIs was only slowed down after the third SuSM peak, according to the PlanetScope NDVI and GCC. The NDWI suggested that the water never reaches the base-level during the dry season as it did in the previous years. The base-level is the relatively stable VI value during the dry periods, Which is during the start and end of the hydrological years of this thesis.

After the first SuSM peak of 2021, VIs reacted immediately and reached similar levels as the year before. The difference was that the water availability of 2021 was substantially smaller than it was during 2020. The water availability was more similar to 2017, although the VI values are not. Another difference is that vegetation reacted directly after the first SuSM peak and not after the second as it did during the previous 4 years. The closed shrubland had the highest VI values, both the grasslands were similar except during the third SuSM peak where only grassland S did not dip very much with the MBI and did not peak very much with the NDWI.

4.2 Selela

4.2.1 Water availability

The water availability is a combination of SuSM, SSM and precipitation, it gives a proper indication of how water is available in the soil and how much fell during precipitation events per year. The SuSM time-series of Manyara Ranch is seen in figure 12. The SSM time-series of Manyara Ranch is seen in figure 13. The precipitation time-series of Manyara Ranch is seen in figure 14. All detailed information of the water availability of Manyara Ranch is seen in table 4.

While the rains were already falling at the beginning of 2017, the SuSM threshold was only reached in February and the SSM threshold only in March. There was little water availability with just 281.7 mm of precipitation.

The rains of 2018 started approximately 2 weeks before the SuSM and SSM reached their threshold. After each precipitation event, the SuSM and SSM reacted.

The SuSM and SSM only reacted in 2019 after 1.5 months of precipitation. Precipitation started in mid-October and the SuSM and SSM only reached their threshold in December. Precipitation was not constant, it was scattered and resulted in high intensity precipitation events. 2019 had an average precipitation rate of 11.8 mm/rain day, which was the second-highest rate for Selela.

A small precipitation event in October resulted in a small peak that reached the threshold for SuSM in 2020. The heavy rains in November resulted in high SuSM and SSM values where the SuSM values remained above the threshold until June. 2020 is the year with the highest water availability in Selela.

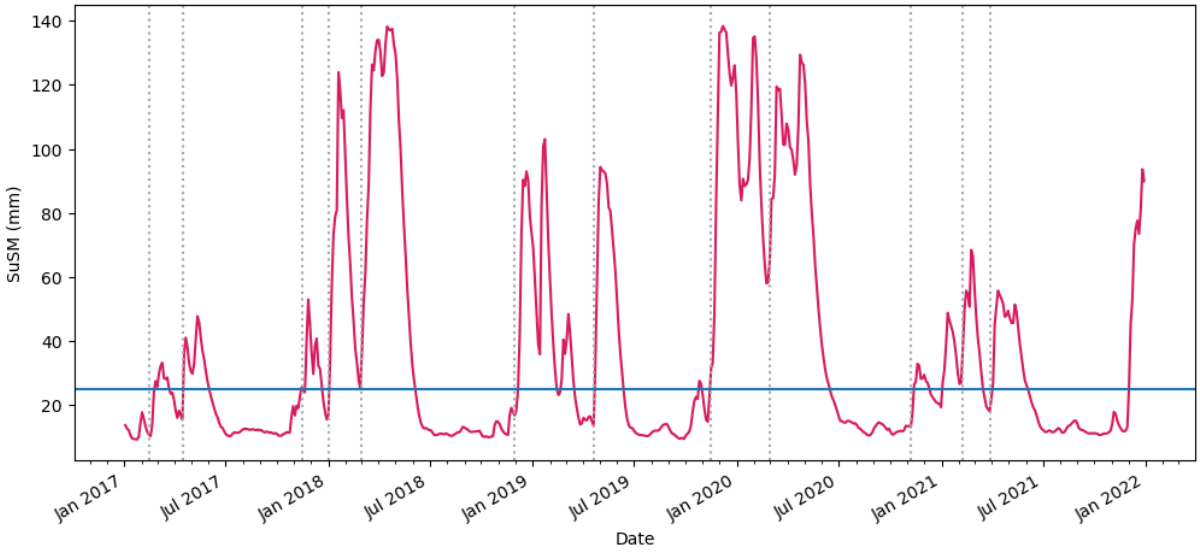

Figure 12; The averaged Subsurface Soil Moisture defined by the SMAP dataset of the Selela ROI. The blue line indicates the threshold at 25 mm at which vegetation could be severely stressed. The onset of a strong increase in Subsurface Soil Moisture is represented by the vertical, grey-dotted lines.

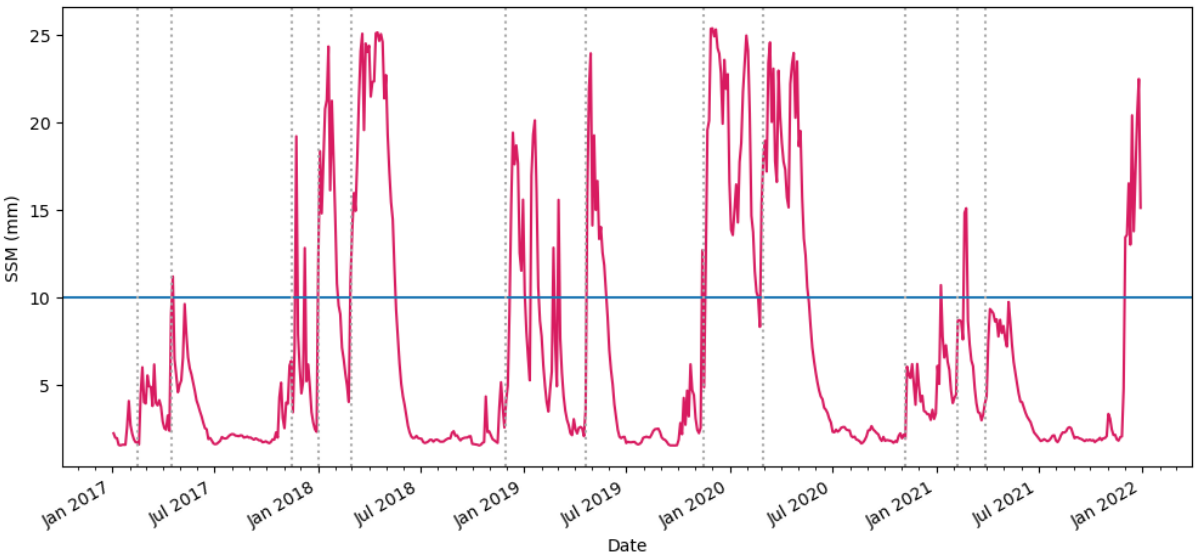

Figure 13; The averaged Surface Soil Moisture defined by the SMAP dataset of the Selela ROI. The blue line indicates the threshold at 10 mm at which vegetation could be severely stressed. The onset of a strong increase in Subsurface Soil Moisture is represented by the vertical, grey-dotted lines.

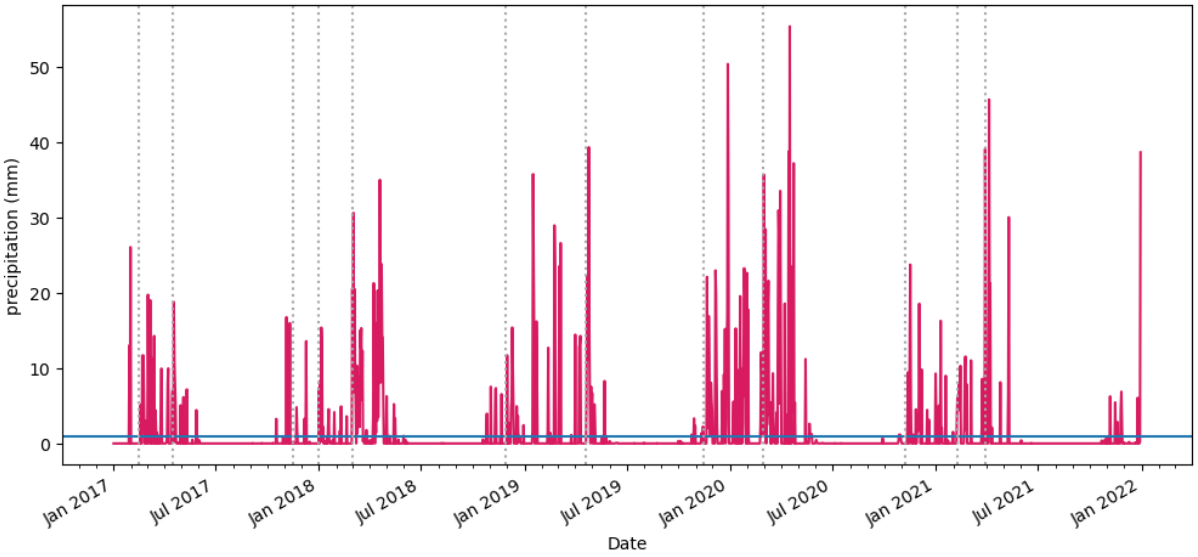

Figure 14; The averaged precipitation defined by the CHIRPS 2.0 dataset of the Selela ROI. The blue line indicates the threshold at 1 mm at which precipitation does not contribute to Subsurface Soil Moisture. The onset of a strong increase in Subsurface Soil Moisture is represented by the vertical, grey-dotted lines.

In 2021 the rains resulted in peaks in the SuSM that reached the threshold. However, the SSM threshold was only reached twice in 2021. After every precipitation event, the SuSM reached the threshold, while the SSM did not.

4.2.2 The whole ROI

During the first overall vegetation degradation assessment of Selela, VIs reacted most of the time after a peak in SuSM, which is shown as a dotted line in figure 10. The only time it did not react was during 2018. The index pattern for NDVI and GCC was similar every year.

In 2017, the VI peak was the second-lowest and thin for NDVI and GCC. The NDVI and GCC reacted after the first SuSM peak and declined quickly afterward. The dip of the MBI and the peak of the NDWI were the third highest. 2017 was the year with the least amount of water availability, yet the NDVI and GCC had the second-lowest peak. Yet, it was contrasting that the MBI and NDWI had such large peaks.

The first two SuSM peaks of 2018, only resulted in a small increase in NDVI and GCC. The third SuSM peak resulted in the third-highest peak for NDVI and GCC, the second-highest dip in MBI and the highest peak in NDWI. The highest dip for MBI had no other indicator that suggested some change in vegetation.

The year 2019 was the year with the third-highest water availability. However, based on VI values, it was the year with the lowest VI values. All VIs reacted after a SuSM peak, but they were all low. It indicated almost no vegetation growth in 2019, even though based on SuSM, SSM and precipitation enough water was available. Although, the NDWI does not indicate enough amounts of water.

Since 2020 was the year with the highest water availability, it was not remarkable that the NDVI and GCC were indicating the highest peaks, thus the most vegetation. VIs reacted directly after the first SuSM peak and had a little peak after the second SuSM peak. The decline in vegetation was slow and based on the NDVI, it never reached the base-level during the dry period. NDWI also did not reach the base-level during the dry period. This suggested that there was some vegetation during the dry period compared to other study years.

The NDVI and GCC values of 2021 were increasing rapidly after the first SuSM peak and were at the maximum just after the second SuSM peak. This maximum resulted in the

second-highest peak, even though 2021 was the second-lowest year for water availability. The dip of MBI and the peak of NDWI were the second-lowest for the whole study period. Thus the VI values of 2021 were higher than in other years, yet there was the least amount of water availability compared to other years.

4.2.3 The 4 vegetation ROIs

The indices derived from Sentinel-2 and PlanetScope for these four areas are given in figure 15.

After the first SuSM peak in 2017, the closed shrubland and savannah had the same vegetation response. Grassland S had a much better response than grassland N, which only had a small response to the SuSM peak. After the second SuSM peak, there was no new VI peak. All VIs declined after the second SuSM peak.

In the second-highest year for water availability, 2018, there were only small or temporary increases in the indices derived from Sentinel-2 for all locations after the first two SuSM peaks. PlanetScope NDVI and GCC were implying a slight increase in vegetation after the second SuSM peak. VIs reacted fast after the third SuSM peak, where closed shrubland and savannah reacted at approximately the same time and both the grasslands later. Closed shrubland had the highest VI values, grassland S and the savannah had approximately the same VI reaction, yet savannah had more. Grassland N had the VI values.

After the first SuSM peak of 2019 the closed shrubland reacted fast, this was seen in all VIs from both satellites. The savannah area reacted a little for both NDVIs, but not for the other indices. Both grasslands did have a small response to the SuSM peak. Savannah reacted better after the second SuSM peak, while the other vegetation types react worse. Thus, only closed shrubland had a normal response and the other three areas lacked a

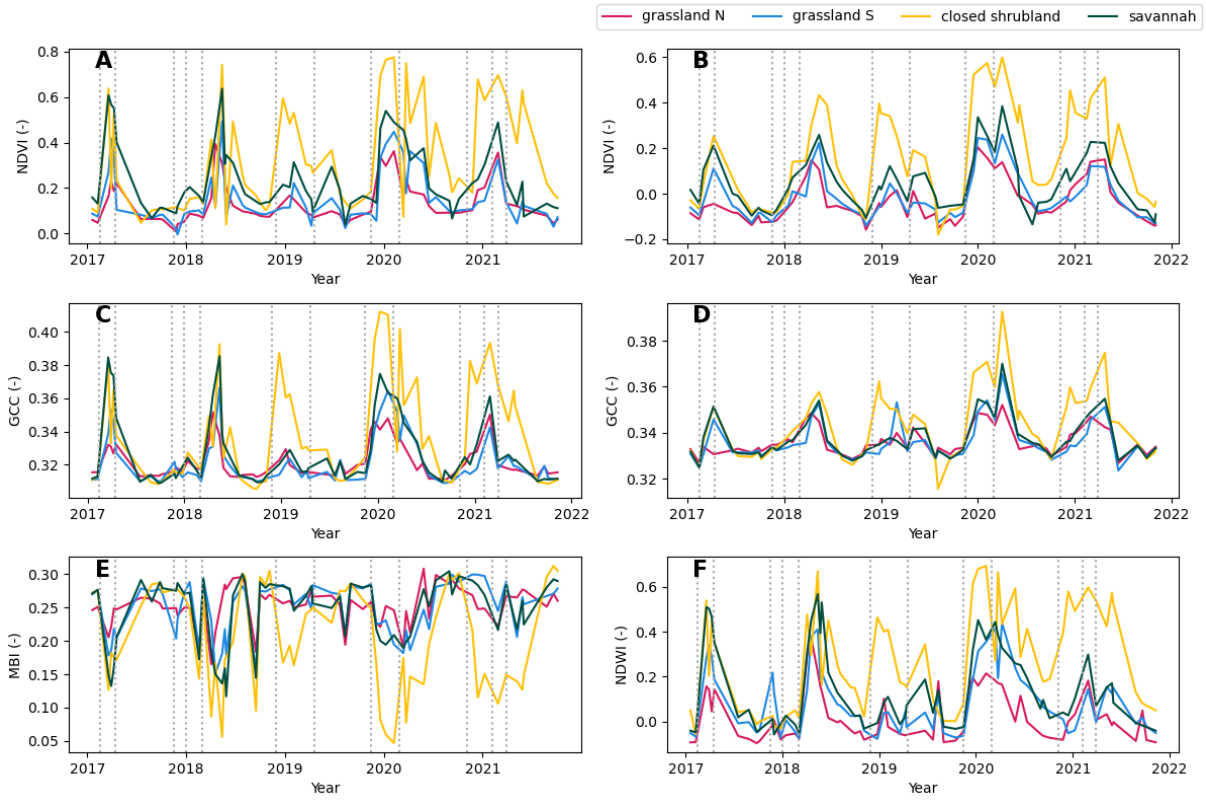

Figure 15; The VI graphs for grassland N, grassland S, closed shrubland and savannah vegetation ROIs inside the Selela ROI. (A) Indicates the NDVI derived from Sentinel-2, (B) indicates the NDVI derived from PlanetScope, (C) indicates the GCC derived from Sentinel-2, (D) indicates the GCC derived from PlanetScope, (E) indicates the MBI derived from Sentinel-2 and (F) indicates the NDWI derived from Sentinel-2. The onset of a strong increase in Subsurface Soil Moisture is represented by the vertical, grey-dotted lines.

proper response. This resulted in the lowest VI value year for both the grasslands and the savannah. This was contrasting since 2019 was the third highest year based on water availability.

With the most water availability, 2020 is the wettest year in Selela. VIs reacted directly after the first SuSM peak. All indices indicate that there was much closed shrubland, it had the highest peak during the study period. The other three areas were also at their highest peak. Of these three, savannah had the highest VI values, followed by grassland S and then by grassland N. Due to the high water availability, the NDWI levels during the dry period did not reach the base-level, except for grassland N at the end of the dry period. The NDVI values from both satellites for closed shrubland did also not reach the base-level during the dry period, suggesting that there was still vegetation during the dry period in 2020 in the closed shrubland.

VIs reacted immediately after the first SuSM peak in 2021. The closed shrubland reached the highest values compared to the other three areas in Selela for all given VIs, thus there was a lot of vegetation. The savannah reacted a little better than the grasslands. Both grasslands reacted similarly. During the second and third peak, VIs reacted again and based on the PlanetScope levels they even reached higher values than after the first VI peak. This only occurred during this year, during the other years the second vegetation peak was never higher than the first vegetation peak. However, Sentinel-2 NDVI and GCC suggested that the VI peaks are similar to or a little lower than the first VI peak after the second and third SuSM peak. Yet, this was still not observed in other study years. This is remarkable since 2021 is the second-lowest year for water availability and it had more closed shrubland and similar savannah and grassland VI values as the years 2018 and 2019, which had a higher water availability.

4.3 LMNP

4.3.1 Water availability

The water availability is a combination of SuSM, SSM and precipitation, it gives a proper indication of how water is available in the soil and how much fell during precipitation events per year. The SuSM time-series of Manyara Ranch is seen in figure 16. The SSM time-series of Manyara Ranch is seen in figure 17. The precipitation time-series of Manyara Ranch is seen in figure 18. All detailed information of the water availability of Manyara Ranch is seen in table 4.

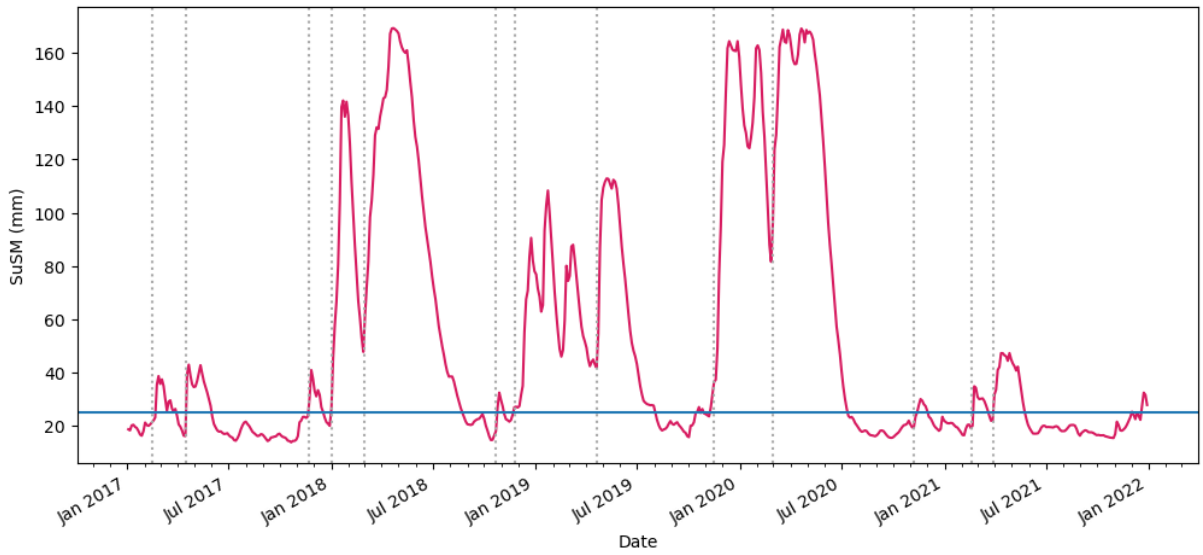

Figure 16; The averaged Subsurface Soil Moisture defined by the SMAP dataset of the LMNP ROI. The blue line indicates the threshold at 25 mm at which vegetation could be severely stressed. The onset of a strong increase in Subsurface Soil Moisture is represented by the vertical, grey-dotted lines.

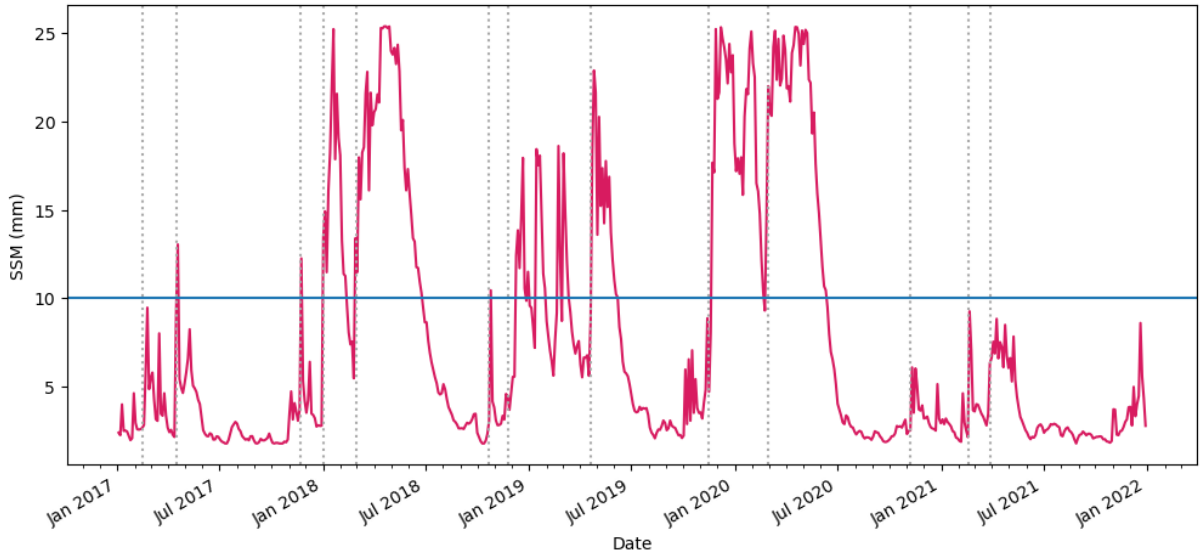

Figure 17; The averaged Surface Soil Moisture defined by the SMAP dataset of the LMNP ROI. The blue line indicates the threshold at 10 mm at which vegetation could be severely stressed. The onset of a strong increase in Subsurface Soil Moisture is represented by the vertical, grey-dotted lines.

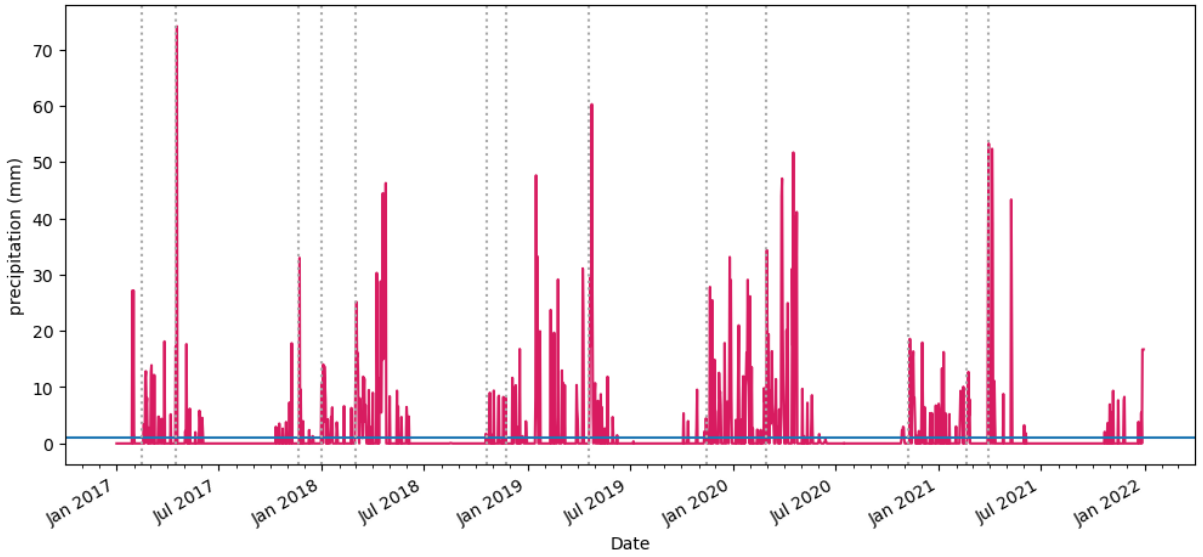

Figure 18; The averaged precipitation defined by the CHIRPS 2.0 dataset of the LMNP ROI. The blue line indicates the threshold at 1 mm at which precipitation does not contribute to Subsurface Soil Moisture. The onset of a strong increase in Subsurface Soil Moisture is represented by the vertical, grey-dotted lines.

In 2017 the SuSM reacted to the precipitation most of the time. SuSM did not react to the high precipitation event of over 70 mm of rain in one day. The SSM peak of that day was also lower than expected. Compared to the amount of precipitation of that day, the SuSM and SSM responses were low.

The SuSM and SSM in 2018 reacted simultaneously with the start of the precipitation event. The peaks of the SuSM and SSM are high compared to the amount of precipitation, especially if compared to the heavy rainfall event of 2017 where the SuSM and SSM did not respond this much.

In 2019 the continuous rains of November only resulted in a small peak for SuSM and SSM. The SuSM reached its threshold for the second time in December and did not go below it until June.

The little amount of rain in 2020 in October resulted in a small peak for SuSM and SSM. When the heavy rain started in the middle of November, the SuSM reached its threshold

and it did not come below it until July. 2020 is the year with the highest water availability in LMNP.

2021 never reached the SSM threshold, even though precipitation did not lack in 2021. The SuSM value kept moving around the threshold and followed the temporal precipitation pattern.

4.3.2 The whole ROI

During the first overall vegetation degradation assessment of LMNP, VIs reacted after a peak in SuSM, which is shown as a dotted line in figure 10. Both NDVI and GCC were having a higher base-level for LMNP compared to Manyara Ranch and Selela. However, the relative peaks were also lower. The MBI was much lower compared to Manyara Ranch and Selela and the NDWI was much higher. This indicated more water and less vegetation variation. However, this was biased because of Lake Manyara, which covers a large amount of the LMNP ROI.

After the first SuSM peak in 2017 vegetation reacted fast in LMNP. There was a small VI peak just before the second SuSM peak, which was related to the heavy precipitation event (>70 mm/day), and a delayed peak after the second SuSM peak. This was observed in all VIs. During the dry period after the late vegetation peak, the MBI was higher than the starting MBI and the NDWI was lower than the start value. This indicated that there was more bare soil and less water at the end of 2017 than at the beginning.

The first and second SuSM peak of 2018 resulted in a small peak in NDVI, GCC and NDWI. Only the first SuSM peak resulted in a small dip for MBI and the second SuSM peak resulted in a larger dip for MBI. After the third SuSM peak, the VI values peaked again for a month. After this period the NDVI and GCC declined and NDWI increased and MBI decreased. This suggested an increase in water, which seems legit since 2018 was the second-highest year of water availability.

In 2019 VIs peaked directly after the two SuSM peaks. According to the MBI and GCC the second peak, thus after the second SuSM peak, resulted in less vegetation. However, NDVI and NDWI suggested that the amount of vegetation was approximately similar. During the dry period of 2019, GCC was higher than the base-level, MBI was higher than at the start of 2019, and NDWI was also higher than at the start of 2019.

2020 started with a VI peak after the first SuSM peak. After this first VI peak, there was another VI peak before the second SuSM peak. However, there was a small related SuSM peak. After the second SuSM peak, there was a decline in NDVI and GCC and an increase in NDWI. This is due to an increase in Lake Manyara; thus, the results were biased. The NDVI, MBI and NDWI are implying there is less vegetation, yet there is just more lake. GCC is not affected by the increase of Lake Manyara and returns to the base-level during the dry period. It was not remarkable Lake Manyara is increasing since it is a terminal lake and 2020 is the wettest year.

The SuSM threshold was never reached during 2021, thus small SuSM peaks were chosen. VI values peaked after the first SuSM peak, this was observed in all indices. According to the NDVI, MBI and NDWI vegetation peaked after the third SuSM peak, this was only minimally observed in the GCC.

4.3.3 The 2 vegetation ROIs

The indices derived from Sentinel-2 and PlanetScope for these two areas are given in figure 19. Both vegetation types reacted the same after SuSM peaks, the only difference was that forest had more vegetation and thus higher VI values. As seen in the even base-level of the NDWI, MBI and NDVI Lake Manyara did not directly affect these two areas.

Except for the PlanetScope based GCC, all VIs indicated an increase in value after both the SuSM peaks of 2017, where the VI was at its maximum after the second SuSM peak.

The VIs reacted fast after the first SuSM peak of 2018. Both the GCC indices suggested that vegetation peaked at its maximum after the first SuSM peak, while both the NDVI

indices suggested that the vegetation peak is after the third SuSM peak. This vegetation peak after the third SuSM peak was seen in all indices and was linked with the precipitation events that occur.

During the third lowest water availability year, 2019, VIs only peaked after the two SuSM peaks. The SuSM peaks did not respond to large increases of VI and the VIs declined fast afterward. Vegetation was relatively low, compared to the water availability.

During the year with the highest water availability, the VIs started increasing just before the first SuSM peak and kept increasing until the second SuSM peak. The decline of VI values was slow after the second SuSM peak. The NDWI during the dry period was different for forest and closed shrubland, forest reaches the base-level while closed shrubland did not reach this base-level.

The response of closed shrubland was faster than forest after the first SuSM peak of 2021. VIs peaked after the second SuSM peak. After the third SuSM peak, the VIs reacted properly again. The high VI values were remarkable for 2021 since it was the year with the second-lowest water availability.

5 Discussion

5.1 Interesting years

The years that were contrasting with other years are called interesting years. These interesting years could give an indication for vegetation degradation or it could be the reason VIs react as they do. First, the interesting years of water availability are discussed, after that the interesting VI years are considered.

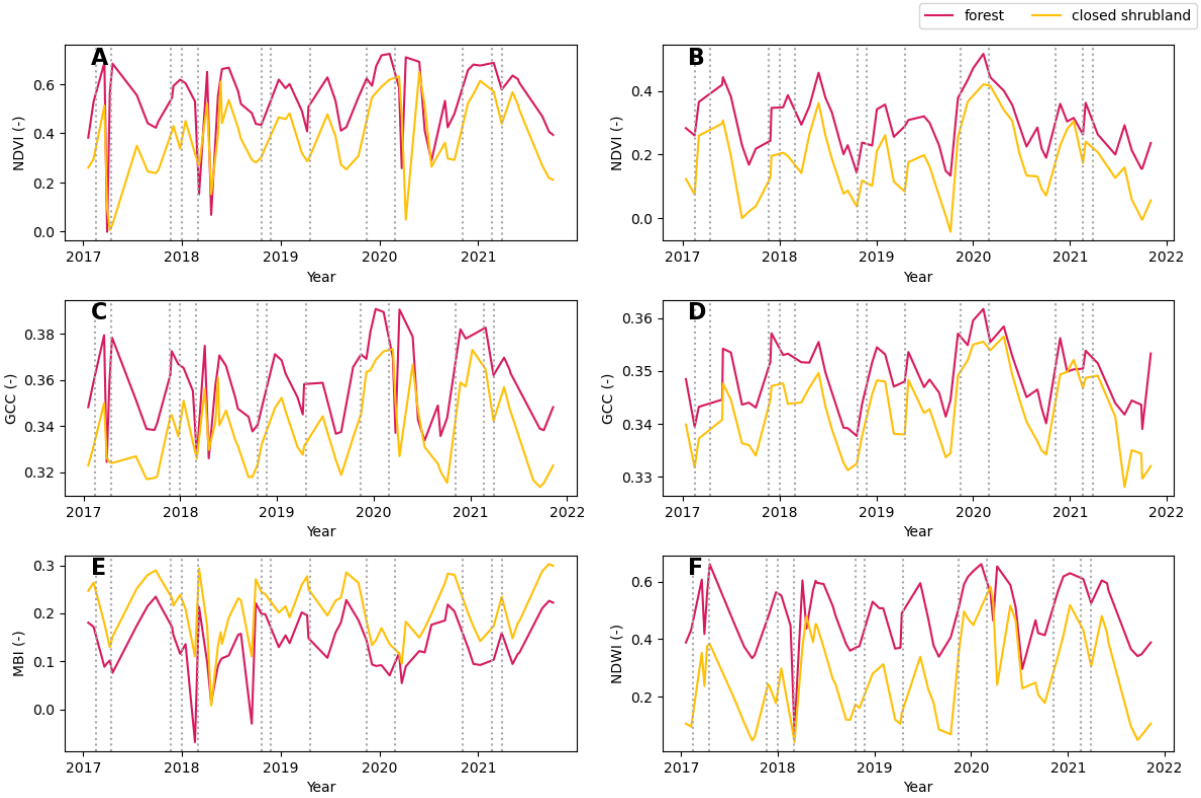

Figure 19; The VI graphs for forest and closed shrubland vegetation ROIs inside the LMNP ROI. (A) Indicates the NDVI derived from Sentinel-2, (B) indicates the NDVI derived from PlanetScope, (C) indicates the GCC derived from Sentinel-2, (D) indicates the GCC derived from PlanetScope, (E) indicates the MBI derived from Sentinel-2 and (F) indicates the NDWI derived from Sentinel-2. The onset of a strong increase in Subsurface Soil Moisture is represented by the vertical, grey-dotted lines.

5.1.1 Manyara Ranch

Based on water availability there are no interesting years for Manyara Ranch. This is because when precipitation falls, the SSM and SuSM are also going up. This indicates normal infiltration in Manyara Ranch.

2018 is an interesting year since vegetation only peaks after the third SuSM peak. This is during the dry period. During the same period, the NDWI, SuSM and SSM are also at their maximum value over the whole study period. This suggests a saturated soil.

Other interesting years are 2019 and 2021. This is because all indices suggest that there is more vegetation in 2021 than in 2019, while 2021 is a much drier year. The SuSM of 2019 (4191.9 mm) lasted 177 days and the SuSM of 2021 (2816.0 mm) lasted 72 days. The SSM of 2019 (756.7 mm) lasted 75 days and the SSM of 2021 (468.8 mm) lasted just 3 days. The precipitation of 2019 (639.2 mm) and 2021 (533.8 mm) lasted a similar time (respectively 59 vs 52 days). This suggests that 2021 had a higher infiltration rate since there are almost no SSM days. However, the infiltration during 2019 is not worse since it still has more SuSM days than in 2021.

5.1.2 Selela

In 2019 when the precipitation starts in Selela, it takes some time for the SuSM to react to it, also the SSM does not react as soon as the precipitation starts. This indicates a lack of infiltration. A comparable situation occurs in 2018, yet to a smaller extent.

The vegetation pattern in Selela in 2018 is similar to that in Manyara Ranch, which is described in section 4.1.4.

Other interesting years are 2019 and 2021. This is because all indices suggest that there is more vegetation in 2021 than in 2019, while 2021 is a much drier year. The SuSM of 2019 (3980.0 mm) lasted 144 days and the SuSM of 2021 (3210.3 mm) lasted 168 days. The SSM of 2019 (731.3 mm) lasted 84 days and the SSM of 2021 (553.9 mm) lasted 9 days. The precipitation of 2019 (545.4 mm) and 2021 (469.8 mm) lasted a similar time (respectively 48 vs 52 days). Thus, the water availability was higher in 2019, yet there are more SuSM days in 2021 and significantly fewer SSM days. This suggests that 2021 had a higher infiltration rate and even more infiltration than 2019.

5.1.3 LMNP

While looking at the two areas in LMNP, no interesting years are identified. All years react to the precipitation and SuSM as suspected. Water is in abundance and vegetation reacts fast to an input of water.

5.2 Crusting theory

The study period started with the driest year, 2017. This provides proper weather conditions for a possible cause of the remarkable vegetation patterns that are not in line with precipitation events, namely crusting. Bare and grazed soils are more prone to crusting than soils under vegetation (Assouline et al., 2015; Kidron et al., 2017; Mills & Fey, 2004), this could explain why Selela was more affected by the remarkable temporal vegetation pattern than LMNP.

The little precipitation in 2017 could cause crust formation on the soil. This is seen with the first precipitation of 2018, where little to no vegetation starts to grow. The little infiltration causes overland flow and spreads the nutrients formed in the biological crust over the area. The precipitation reaches an extreme, which causes floods in the area (IFRC, 2018). These floods could be an explanation for the lack of vegetation. After the floods, when the nutrients from the biological crust are scattered over the area (Belnap et al., 2005), vegetation growth starts to boost as is seen in the graphs for all ROIs and the small areas within. During this vegetation boost, animals and livestock use this opportunity after the long lack of vegetation to eat. This sudden increase and trampling on the moist soil

causes new conditions for physical crust formation (Assouline et al., 2015; Runnström et al., 2019).

When the precipitation starts in 2019, it takes approximately 3 weeks before the SuSM, SSM and NDWI react. This means it takes some time for water to infiltrate the soil. This is because of the physical crusting which limits the infiltration. Physical crusting can slow the grass growth (Sankaran, 2019), yet it has less effect on trees and shrubs (Bond, 2008; Mills & Fey, 2004; Sankaran et al., 2004; Scholes & Archer, 1997). This is noticeable in the Selela closed shrublands and probably on the savannah where the few shrubs react faster. The grasses have a delayed and lower growth in Selela due to the physical crusting. The late vegetation might be quickly eaten by livestock of the Maasai, this can be an explanation for the low grassland peaks. A similar growth pattern is seen in Manyara Ranch where the closed shrublands react better to the SuSM peak than the grasslands. However, less livestock is allowed in Manyara Ranch and this results in less physical crusting and less, peak limiting, grazing. This is in line with the observations of Manyara Ranch.

The precipitation of 2020 starts with a high intensity event and right after this event, the SuSM and SSM peaks occurred. Thus, if there was any crusting, it is removed due to this event or there was no crusting during the start of 2020. In 2020 there was a lot of infiltration and the soil was saturated. This resulted in the observed boost of vegetation. The soil was so saturated, that during the dry period the soil did not dry out as was seen by the NDWI values. Due to this, crust formation was not possible.

As a result of the lack of crust at the start of the precipitation of 2021, the SuSM peak was simultaneous with the first precipitation. The SSM peak lacked since infiltration was high due to the lack of a soil crust. This higher than 'normal' infiltration resulted in the remarkable high vegetation during 2021 with relatively little precipitation.

That crusting is the cause of the remarkable vegetation patterns is nothing but a theory since no hard evidence is found in the field. To confirm this theory, fieldwork is needed in the studied areas. This must be done before the first rain to confirm any crusting and to study the resilience. Other explanations that could be the result are differences in grazing types (Sankaran, 2019) or even fires that affect the growth of vegetation (Bond, 2008; Okello et al., 2008; Sankaran, 2019; Sankaran et al., 2004).

Even the theory of the crusting itself can be different since crusting can have positive as well as negative effects on vegetation (Assouline et al., 2015). One type of crust can have many different effects on the growing vegetation which can change even locally (Mills & Fey, 2004), which can result in different results of vegetation growth or vegetation degradation. An example of different crusting results in savannah areas are the 'moving' banded vegetation patterns, like the tiger bush patterns (Lefever & Lejeune, 1997; Thiery et al., 1995).

Even with the crusting, vegetation reacts fast to an increase in SuSM. This means that the vegetation resilience is still very high, which is in line with the study of Verhoeve et al. (2021). Even though the vegetation resilience is high, it does not mean that there is no vegetation degradation. However, this thesis was too short to observe vegetation degradation. Yet, some signs of vegetation degradation are observed during this thesis. Due to the crusting, shrubs and trees are observed to have a higher resilience than grasses. This means that woody vegetation has a better survival in savannah areas, this is in line with the findings of bush encroachment (H. S. Kimaro & Treydte, 2021; Li et al., 2020; Mtui et al., 2017; Stevens et al., 2017; Venter et al., 2018) and the observations made by the Maasai itself (Verhoeve, 2019).

6 Conclusion

Using SuSM, SSM and precipitation data together provides a proper indication for water availability and infiltration. In combination with the VIs derived from Sentinel-2, it gives a good estimation of vegetation growth in the ROIs. Yet, it does not provide detailed information about vegetation types. Using CCDC, highly variable areas can be located inside the ROI. These areas are studied in more detail with the PlanetScope derived VIs.

With the more detailed assessment, it is observed that crusting might be affecting the vegetation in both a positive (the nutrient-rich biological crusting) and in a negative (the infiltration limiting physical crusting) way. It is observed that vegetation only starts growing with enough SuSM and not when it starts raining. First, the precipitation must remove soil crust for water infiltration, which results in a SuSM peak. If there is a SuSM peak, vegetation grows fast. This indicates that vegetation resilience is high. Less crusting takes place under vegetation, like bushes and trees. This results in a more resilient woody vegetation since infiltration is less limited under the woody vegetation. This observation can result in a longer timeframe for bush encroachment in the savannah areas, which results in less grasses and food for the Maasai livestock. This is the most significant indication of vegetation degradation. However, vegetation degradation itself is not observed due to the short study period.

Recommendation

To study the vegetation degradation in LMNP, Manyara Ranch and Selela, the relationship between crusting and vegetation resilience must be better understood. This can be accomplished with fieldwork and with more temporal analysis with PlanetScope images. This can confirm or deny the crusting theory from this thesis. This fieldwork needs to be done before the first rains since that is the time the soil is possibly crusted. On this crusted soil, infiltration can be studied before the rains, e.g. with the method of (Mills & Fey, 2004) or with a rainfall simulator. After the rains start, observations need to be made to find out if infiltration is occurring or if there is overland flow. Observations on when vegetation starts to grow are also needed. With this data, the resilience can be studied with PlanetScope images. These images need to have as much temporal resolution as possible to study the resilience and the effect of crusting on it. The vegetation can be studied with NDVI and GCC in a similar way as is done in this thesis.

If the crusting theory described in this thesis is correct, bush encroachment can be a major problem for the Maasai and its livestock. Since the nutrient-rich grasses will disappear and change into bushes or trees.

7 References

Assouline, S., Thompson, S. E., Chen, L., Svoray, T., Sela, S., & Katul, G. G. (2015). The dual role of soil crusts in desertification. *Journal of Geophysical Research: Biogeosciences*, *120*(10), 2108–2119. https://doi.org/10.1002/2015JG003185

AWF. (2003). Lake Manyara Watershed Assessment: Progress Report-Lake Manyara Watershed Assessment. *African Wildlife Foundation*, *December*, 1–27.

Belnap, J., Welter, J. R., Grimm, N. B., Barger, N., & Ludwig, J. A. (2005). LINKAGES BETWEEN MICROBIAL AND HYDROLOGIC PROCESSES IN ARID AND SEMIARID WATERSHEDS. *Special Feature Ecology*, *86*(2), 298–307.

Bond, W. J. (2008). What Limits Trees in C4 Grasslands and Savannas? *Http://Dx.Doi.Org.Proxy.Library.Uu.Nl/10.1146/Annurev.Ecolsys.39.110707.173411*, *39*, 641–659. https://doi.org/10.1146/ANNUREV.ECOLSYS.39.110707.173411

Bradford, J., & Huang, C. (1992). Mechanisms of crust formation: physical components. In M. Sumner & B. Stewart (Eds.), *Soil crusting: chemical and physical processes* (pp. 55–72). Lewis Publishers Boca Raton FL.

Cheng, Y., Vrieling, A., Fava, F., Meroni, M., Marshall, M., & Gachoki, S. (2020). Phenology of short vegetation cycles in a Kenyan rangeland from PlanetScope and Sentinel-2. *Remote Sensing of Environment*, *248*, 112004. https://doi.org/10.1016/j.rse.2020.112004

Compen, V. L. P. (2021). *The shrinkage of Lake Manyara: causes and management options for lake protection*. http://dspace.library.uu.nl/handle/1874/406231

Conroy, A. B. (2001). Maasai oxen, agriculture and land use change in Monduli District, Tanzania. *ProQuest Dissertations and Theses*, *3006129*(University of New Hampshire), 547. https://scholars.unh.edu/dissertation

Cooke, A. E., Leslie, P. W., Meade, M., Reice, S., White, P. S., & Withmore, T. (2007). *Subdividing the savanna: The ecology of change in northern Tanzania*. *3272780*, 245. http://0-search.proquest.com.wam.leeds.ac.uk/docview/304830771?accountid=14664%0Ahttp://openurl.ac.uk/?genre=dissertations+%26+theses&issn=&title=Subdividing+the+savanna%3A+The+ecology+of+change+in+northern%0ATanzania&volume=&issue=&date=2007-01-01&atitle

Degen, J. (2015). *Impact of land cover and soil conservation on soil erosion rates in the Tikur Woha Catchment, Ethiopia*.

Deus, D., Gloaguen, R., & Krause, P. (2013). Water balance modeling in a semi-arid environment with limited in situ data using remote sensing in lake manyara, east african rift, tanzania. *Remote Sensing*, *5*(4), 1651–1680. https://doi.org/10.3390/rs5041651

Egberts, N. (2020). *Analyzing gully erosion in the Lake Manyara catchment– Tanzania*. http://dspace.library.uu.nl/handle/1874/404675

Entekhabi, D., Njoku, E. G., O'Neill, P. E., Kellogg, K. H., Crow, W. T., Edelstein, W. N., Entin, J. K., Goodman, S. D., Jackson, T. J., Johnson, J., Kimball, J., Piepmeier, J. R., Koster, R. D., Martin, N., McDonald, K. C., Moghaddam, M., Moran, S., Reichle, R., Shi, J. C., … Van Zyl, J. (2010). The soil moisture active passive (SMAP) mission. *Proceedings of the IEEE*, *98*(5), 704–716. https://doi.org/10.1109/JPROC.2010.2043918

ESA. (n.d.-a). *Level-1C Processing - Sentinel-2 MSI Technical Guide - Sentinel Online - Sentinel Online*. Retrieved October 20, 2021, from https://sentinels.copernicus.eu/web/sentinel/technical-guides/sentinel-2-msi/level-1c-processing

ESA. (n.d.-b). *MSI Instrument – Sentinel-2 MSI Technical Guide – Sentinel Online - Sentinel Online*. Retrieved October 20, 2021, from https://sentinels.copernicus.eu/web/sentinel/technical-guides/sentinel-2-msi/msi-instrument

ESA. (n.d.-c). *Sentinel-2 - Missions - Sentinel Online - Sentinel Online*. Retrieved October 20, 2021, from https://sentinel.esa.int/web/sentinel/missions/sentinel-2

Fratkin, E. (2001). East African Pastoralism in Transition: Maasai, Boran, and Rendille Cases. *African Studies Review*, *44*(3), 1–25. https://doi.org/10.2307/525591

Funk, C., Peterson, P., Landsfeld, M., Pedreros, D., Verdin, J., Shukla, S., Husak, G., Rowland, J., Harrison, L., Hoell, A., & Michaelsen, J. (2015). The climate hazards infrared precipitation with stations - A new environmental record for monitoring extremes. *Scientific Data*, *2*(1), 1–21. https://doi.org/10.1038/sdata.2015.66

Gao, B. C. (1996). NDWI—A normalized difference water index for remote sensing of vegetation liquid water from space. *Remote Sensing of Environment*, *58*(3), 257–266. https://doi.org/10.1016/S0034-4257(96)00067-3

Gillespie, A. R., Kahle, A. B., & Walker, R. E. (1987). Color enhancement of highly correlated images. II. Channel ratio and "chromaticity" transformation techniques. *Remote Sensing of Environment*, *22*(3), 343–365. https://doi.org/10.1016/0034-4257(87)90088-5

Goldman, M. J. (2011). Strangers in their own land: Maasai and wildlife conservation in Northern Tanzania. *Conservation and Society*, *9*(1), 65–79. https://doi.org/10.4103/0972-4923.79194

Hadeel, A., Jabbar, M., & Chen, X. (2012). Remote sensing and GIS application in the detection of environmental degradation indicators. *Http://Www.Tandfonline.Com/Action/JournalInformation?Show=aimsScope&journalCode=tgsi20#.VsXpLiCLRhE*, *14*(1), 39–47. https://doi.org/10.1007/S11806-011-0441-Z

Hawkes, C. V. (2003). NITROGEN CYCLING MEDIATED BY BIOLOGICAL SOIL CRUSTS AND ARBUSCULAR MYCORRHIZAL FUNGI. *Ecology*, *84*(6), 1553–1562.

Homewood, K., Kristjanson, P., & Trench, P. C. (2009). *Changing Land Use, Livelihoods and Wildlife Conservation in Maasailand* (pp. 1–42). https://doi.org/10.1007/978-0-387-87492-0_1

IFRC. (2018, April 30). *Tanzania: Floods - Emergency Plan of Action, DREF operation n° MDRTZ021 - United Republic of Tanzania | ReliefWeb*. https://reliefweb.int/report/united-republic-tanzania/tanzania-floods-emergency-plan-action-dref-operation-n-mdrtz021

Iqbal, M. F., & Khan, I. A. (2014). Spatiotemporal Land Use Land Cover change analysis and erosion risk mapping of Azad Jammu and Kashmir, Pakistan. *Egyptian Journal of Remote Sensing and Space Science*, *17*(2), 209–229. https://doi.org/10.1016/j.ejrs.2014.09.004

Keijzer, T. (2020). *Drought Analysis of the Lake Manyara Catchment: Meteorological Drought Occurence, Influence of Atmospheric Teleconnections and Impact on Lake Manyara*. http://dspace.library.uu.nl/handle/1874/402494

Kidron, G. J., Ying, W., Starinsky, A., & Herzberg, M. (2017). Drought effect on biocrust resilience: High-speed winds result in crust burial and crust rupture and flaking. *The Science of the Total Environment*, *579*, 848–859. https://doi.org/10.1016/j.scitotenv.2016.11.016

Kimaro, E. G., Mor, S. M., & Toribio, J.-A. L. M. L. (2018). Climate change perception and impacts on cattle production in pastoral communities of northern Tanzania. *Pastoralism 2018 8:1*, *8*(1), 1–16. https://doi.org/10.1186/S13570-018-0125-5

Kimaro, H. S., & Treydte, A. C. (2021). Rainfall, fire and large-mammal-induced drivers of Vachellia drepanolobium establishment: Implications for woody plant encroachment in Maswa, Tanzania. *African Journal of Ecology*, *00*, 1–10. https://doi.org/10.1111/AJE.12881

Kiunsi, R. B., & Meadows, M. E. (2006). Assessing land degradation in the Monduli District, northern Tanzania. *Land Degradation and Development*, *17*(5), 509–525. https://doi.org/10.1002/LDR.733

Lefever, R., & Lejeune, O. (1997). On the origin of tiger bush. *Bulletin of Mathematical Biology*, *59*(2), 263–294. https://doi.org/10.1007/BF02462004

Li, W., Buitenwerf, R., Munk, M., Bøcher, P. K., & Svenning, J. C. (2020). Deep-learning based high-resolution mapping shows

woody vegetation densification in greater Maasai Mara ecosystem. *Remote Sensing of Environment*, *247*, 111953. https://doi.org/10.1016/J.RSE.2020.111953
Loth, P. E. (1999). The vegetation of Manyara: scale-dependent states and transitions in the African Rift Valley. In *The vegetation of Manyara: scale-dependent states and transitions in the African Rift Valley.*
Lyu, X., Li, X., Dang, D., Dou, H., Xuan, X., Liu, S., Li, M., & Gong, J. (2020). A new method for grassland degradation monitoring by vegetation species composition using hyperspectral remote sensing. *Ecological Indicators*, *114*, 106310. https://doi.org/10.1016/J.ECOLIND.2020.106310
Maerker, M., Quénéhervé, G., Bachofer, F., & Mori, S. (2015). A simple DEM assessment procedure for gully system analysis in the Lake Manyara area, northern Tanzania. *Natural Hazards*, *79*(1), 235–253. https://doi.org/10.1007/s11069-015-1855-y
Manyara Ranch Conservancy. (2019). *Area Information - Manyara Ranch Conservancy - Tanzania*. https://manyararanch.com/area-information/
Mayland, H. F., & McIntosh, T. H. (1966). Availability of Biologically Fixed Atmospheric Nitrogen-15 to Higher Plants. *Nature 1966 209:5021*, *209*(5021), 421–422. https://doi.org/10.1038/209421A0
McCabe, J. T., Leslie, P. W., & DeLuca, L. (2010). Adopting Cultivation to Remain Pastoralists: The Diversification of Maasai Livelihoods in Northern Tanzania. *Human Ecology 2010 38:3*, *38*(3), 321–334. https://doi.org/10.1007/S10745-010-9312-8
McIntyre, D. S. (1958). *Permeablity of raindrop impacts*.
Meneses-Tovar, C. L. (2011). NDVI as indicator of degradation. *Unasylva (English Ed.)*, *62*(238), 39–46.
Mills, A. J., & Fey, M. V. (2004). Effects of vegetation cover on the tendency of soil to crust in South Africa. *Soil Use and Management*, *20*(3), 308–317. https://doi.org/10.1111/j.1475-2743.2004.tb00375.x
Monduli District Council. (2021). *investment opportunities | Monduli District Council*. http://www.mondulidc.go.tz/investment-oppotunities
Mtui, D. T., Lepczyk, C. A., Chen, Q., Miura, T., & Cox, L. J. (2017). Assessing multi-decadal land-cover – land-use change in two wildlife protected areas in Tanzania using Landsat imagery. *PLoS ONE*, *12*(9). https://doi.org/10.1371/journal.pone.0185468
Nguyen, C. T., Chidthaisong, A., Diem, P. K., & Huo, L.-Z. (2021). A Modified Bare Soil Index to Identify Bare Land Features during Agricultural Fallow-Period in Southeast Asia Using Landsat 8. *Land 2021, Vol. 10, Page 231*, *10*(3), 231. https://doi.org/10.3390/LAND10030231
Niboye, E. P. (2010). Vegetation Cover Changes in Ngorongoro Conservation Area from 1975 to 2000: The Importance of Remote Sensing Images. *The Open Geography Journal*, *3*, 15–27.
Oba, G., & Kaitira, L. M. (2006). Herder knowledge of landscape assessments in arid rangelands in northern Tanzania. *Journal of Arid Environments*, *66*(1), 168–186. https://doi.org/10.1016/J.JARIDENV.2005.10.020
Okello, B. D., Young, T. P., Riginos, C., Kelly, D., & O'Connor, T. G. (2008). Short-term survival and long-term mortality of Acacia drepanolobium after a controlled burn. *African Journal of Ecology*, *46*(3), 395–401. https://doi.org/10.1111/J.1365-2028.2007.00872.X
Pickett, S. T. A., Cadenasso, M. L., & Benning, T. L. (2003). Biotic and abiotic variability as key determinants of savanna heterogeneity at multiple spatiotemporal scales. *The Kruger Experience: Ecology and Management of Savanna Heterogeneity*, 22–40.
Planet. (2021, March 22). *PlanetScope*. https://developers.planet.com/docs/data/planetscope/
Rouse, J. W., Haas, R. H., Schell, J. A., & Deeering, D. . (1973). Monitoring vegetation systems in the Great Plains with ERTS (Earth Resources Technology Satellite). *Third Earth Resources Technology Satellite-1 Symposium*, 309–317.
Runnström, M. C., Ólafsdóttir, R., Blanke, J., & Berlin, B. (2019). Image Analysis to Monitor Experimental Trampling and Vegetation Recovery in Icelandic Plant Communities. *Environments 2019, Vol. 6, Page 99*, *6*(9), 99. https://doi.org/10.3390/ENVIRONMENTS6090099
Sankaran, M. (2019). Droughts and the ecological future of tropical savanna vegetation. *Journal of Ecology*, *107*(4), 1531–1549. https://doi.org/10.1111/1365-2745.13195
Sankaran, M., Ratnam, J., & Hanan, N. P. (2004). Tree-grass coexistence in savannas revisited - Insights from an examination of assumptions and mechanisms invoked in existing models. In *Ecology Letters* (Vol. 7, Issue 6, pp. 480–490). https://doi.org/10.1111/j.1461-0248.2004.00596.x
Scholes, R. J., & Archer, S. R. (1997). TREE-GRASS INTERACTIONS IN SAVANNAS 1. *Annu. Rev. Ecol. Syst*, *28*, 517–561. www.annualreviews.org
Shechambo, F. (2018). Land Use By People Living Around Protected Areas: The Case of Lake Manyara National Park. *Utafiti Journal*, *4*(1). http://www.journals.udsm.ac.tz/index.php/uj/article/view/1255
Sterk, G., & Stoorvogel, J. J. (2020). Desertification–Scientific Versus Political Realities. *Land 2020, Vol. 9, Page 156*, *9*(5), 156. https://doi.org/10.3390/LAND9050156
Stevens, N., Lehmann, C. E. R., Murphy, B. P., & Durigan, G. (2017). Savanna woody encroachment is widespread across three continents. *Global Change Biology*, *23*(1), 235–244. https://doi.org/10.1111/gcb.13409
Subsurface Soil Moisture (corrected with SMAP imagery). (n.d.).
Surface Soil Moisture (corrected with SMAP imagery). (n.d.).
TANAPA. (2020, July 13). *Lake Manyara National Park*. https://storymaps.arcgis.com/stories/10ce7c6dd58f427d8f9748320acb131f
Thiery, J. M., D'Herbes, J.-M., & Valentin, C. (1995). A Model Simulating the Genesis of Banded Vegetation Patterns in Niger. *The Journal of Ecology*, *83*(3), 497. https://doi.org/10.2307/2261602
TMA. (n.d.). *Tanzania Meteorology Agency, Climate Analyses and Applications Map Room*. Retrieved October 13, 2021, from http://maproom.meteo.go.tz/maproom/
Tucker, C. J. (1979). Red and photographic infrared linear combinations for monitoring vegetation. *Remote Sensing of Environment*, *8*(2), 127–150. https://doi.org/10.1016/0034-4257(79)90013-0
UNESCO. (2019). *Lake Manyara Biosphere Reserve, Tanzania*. https://en.unesco.org/biosphere/africa/lake-manyara
Valentin, C., & D'Herbès, J. M. (1999). Niger tiger bush as a natural water harvesting system. *CATENA*, *37*(1–2), 231–256. https://doi.org/10.1016/S0341-8162(98)00061-7
van den Bergh, H. A. J. (2016). *The impacts of Maasai settlement on land cover, meteorological conditions and wind erosion risk in northern Tanzania*. http://dspace.library.uu.nl/handle/1874/349763
van Rosmalen, R. C. (2021). *Land Use and Land Cover Changes in Monduli District, Tanzania: Analysis of multiple classification methods and satellite sensors in order to perform a multi-temporal post-classification change detection analysis in a difficult to map semi-arid savannah la*. http://dspace.library.uu.nl/handle/1874/406211
Venter, Z. S., Cramer, M. D., & Hawkins, H.-J. (2018). Drivers of woody plant encroachment over Africa. *Nature Communications 2018 9:1*, *9*(1), 1–7. https://doi.org/10.1038/s41467-018-04616-8
Verhoeve, S. L. (2019). *Satellite based analysis of environmental changes in the Monduli and Longido districts, Tanzania*. https://dspace.library.uu.nl/bitstream/handle/1874/383352/Thesis.pdf?sequence=2
Verhoeve, S. L., Keijzer, T., Kaitila, R., Wickama, J., & Sterk, G. (2021). Vegetation Resilience under Increasing Drought Conditions in Northern Tanzania. *Remote Sensing 2021, Vol. 13, Page 4592*, *13*(22), 4592.

https://doi.org/10.3390/RS13224592
Wynants, M., Solomon, H., Ndakidemi, P., & Blake, W. H. (2018). Pinpointing areas of increased soil erosion risk following land cover change in the Lake Manyara catchment, Tanzania. *International Journal of Applied Earth Observation and Geoinformation*, *71*, 1–8. https://doi.org/10.1016/j.jag.2018.05.008
Yanda, P. Z., & Madulu, N. F. (2005). Water resource management and biodiversity conservation in the Eastern Rift Valley Lakes, Northern Tanzania. *Physics and Chemistry of the Earth, Parts A/B/C*, *30*(11–16), 717–725. https://doi.org/10.1016/J.PCE.2005.08.013
Yengoh, G. T., Dent, D., Olsson, L., Tengberg Compton, A. E., & Tucker, J. (2014). *The use of the Normalized Difference Vegetation Index (NDVI) to assess land degradation at multiple scales: a review of the current status, future trends, and practical considerations*. www.lucsus.lu.se
Zhu, Z., & Woodcock, C. E. (2014). Continuous change detection and classification of land cover using all available Landsat data. *Remote Sensing of Environment*, *144*, 152–171. https://doi.org/10.1016/J.RSE.2014.01.011